



FEDERAL UNIVERSITY OF SANTA CATARINA  
TECHNOLOGY CENTER  
GRADUATE PROGRAM IN CHEMICAL ENGINEERING

Arthur Santos Romero

**Dry polishing of enzymatically produced fatty acid methyl esters through  
polymeric membrane**

Florianópolis

2022

Arthur Santos Romero

**Dry polishing of enzymatically produced fatty acid methyl esters through  
polymeric membrane**

Master thesis for obtaining the degree of Master's in  
Chemical Engineering presented to the Graduate  
Program in Chemical Engineering at the Federal  
University of Santa Catarina.

Supervisor:  
Prof. Dr. José Vladimir de Oliveira/UFSC

Co-supervisors:  
Prof. Dr. Dachamir Hotza/UFSC  
Prof. Dr. Murilo Daniel de Mello Innocentini/UNAERP

Florianópolis

2022

Ficha de identificação da obra elaborada pelo autor,  
através do Programa de Geração Automática da Biblioteca Universitária da UFSC

Santos Romero, Arthur  
Dry Polishing of Enzymatically Produced Fatty Acid  
Methyl Esters Through Polymeric Membrane / Arthur Santos  
Romero ; orientador, José Vladimir de Oliveira,  
coorientador, Dachamir Hotza, coorientador, Murilo Daniel  
de Mello Innocentini, 2022.  
90 p.

Dissertação (mestrado) - Universidade Federal de Santa  
Catarina, Centro Tecnológico, Programa de Pós-Graduação em  
Engenharia Química, Florianópolis, 2022.

Inclui referências.

1. Engenharia Química. 2. Chemical Engineering  
Industrial Processes. 3. Membrane Separation Process. 4.  
Polishing of Fatty Acid Methyl Esters. I. Oliveira, José  
Vladimir de . II. Hotza, Dachamir. III. Mello Innocentini,  
Murilo Daniel de IV. Universidade Federal de Santa  
Catarina. Programa de Pós-Graduação em Engenharia Química. V.  
Título.

O presente trabalho em nível de Mestrado foi avaliado e aprovado por banca examinadora composta pelos seguintes membros:

Prof. Dr. Marco Di Luccio  
PPGEAL/UFSC

Dr. Guilherme Zin  
Pesquisador/TransferTech

Certificamos que esta é a **versão original e final** do trabalho de conclusão que foi julgado adequado para obtenção do título de Mestre em Engenharia Química.

---

Profa. Dra. Débora de Oliveira  
Coordenadora do PósENQ

---

Prof. Dr. José Vladimir de Oliveira  
Orientador

Florianópolis, 2022

À minha família

## **ACKNOWLEDGMENTS**

It would not be possible here to express with sufficient intensity all my gratitude to those who contributed to the achievement of this goal. I thank my supervisor, Prof. Dr. José Vladimir de Oliveira for the teaching and enthusiasm he transmitted to me and for the support in the realization of the work presented here. I also thank my co-supervisors, Prof. Dr. Dachamir Hotza and Prof. Dr. Murilo Daniel de Mello Innocentini, for their companionship and for always sharing their knowledge and experiences. In particular, to Prof. Dr. Murilo Daniel de Mello Innocentini for learning, companionship, and for fundamental help in directing me to the present master's program.

To the laboratory of the University of Ribeirão Preto, for the research conditions made available, without which it would not be possible to carry out the research activities.

I also thank the industries that supported the development of the project. Thanks to Koch Separation and DuPont for the donation of the membrane sheets as well as Prisma S.A and Olfar S.A for supplying the industrial fatty acid methyl ester samples, and performing characterization analyses of the obtained permeates.

To the Graduate Program in Chemical Engineering and the Federal University of Santa Catarina for the opportunity.

A very special thanks goes to my family, in particular, my parents, René e Leila, and my sister, Beatriz, for the love, care, and support in the most difficult hours.

## RESUMO

Os processos enzimáticos de produção de biodiesel têm despertado grande interesse industrial. A maior vantagem do processo enzimático, quando comparado ao processo químico convencional, é que ele pode usar matéria-prima barata e de baixa qualidade com alto teor de ácidos graxos livres (AGL) e água. Além disso, processos enzimáticos apresentam condições de reação suaves, baixo consumo de energia, fácil recuperação do produto e, portanto, são ambientalmente corretos e têm custos de produção reduzidos. No entanto, um grande desafio para o processo enzimático é separar várias impurezas como sabão, ácido graxo não reagido, álcool residual, água, glicerol livre, catalisador, fósforo, enxofre, mono- di- e triacilgliceróis que são formadas após a reação de esterificação e transesterificação devido à matéria-prima de baixa qualidade para produzir um produto final de biodiesel que atenda aos padrões de comercialização. Com base nisso, são necessárias etapas de polimento de biodiesel para remoção das impurezas. Neste trabalho, propomos a aplicação do processo de separação por membrana no polimento de ésteres metílicos de ácidos graxo (FAME) oriundos de processo enzimático industrial. Seis membranas diferentes, poliamida (NF90, NF245, NF8038), fluoreto de polivinilideno (PVDF), politetrafluoretileno (PTFE) e polietersulfona (PES) foram selecionadas e usadas para filtração do FAME. O FAME industrial bruto foi filtrado em um processo de fluxo cruzado à temperatura ambiente e gradiente de pressão de 3 bar. Parâmetros de permeabilidade para o fluxo de ar, água e biodiesel “on spec” foram avaliados separadamente para cada membrana. Com base no fluxo de permeado e na análise quantitativa do conteúdo nos permeados, o desempenho da membrana foi avaliado. Os resultados obtidos mostraram que a membrana de PES (10 kDa) apresentou o melhor desempenho resultando em isenção de teor de sabão no permeado. Além disso, a membrana de PES foi capaz de reduzir com sucesso a cor, contaminação total e teor de fósforo das amostras de FAME. Acidez e teor de água também foram reduzidos. Portanto, o processo de separação utilizando membrana de PES (10 kDa) é uma alternativa adequada para o polimento de FAME, reduzindo o número de etapas a jusante.

**Palavras-chaves:** Membrana. Processos de Separação. Ester Metílico de Ácidos Graxos. Polimento. Biodiesel.

## RESUMO EXPANDIDO

### Introdução

O crescimento populacional mundial e a consequente exploração dos recursos naturais sem precedentes têm despertado um grande interesse no estudo por fontes alternativas de energia renovável e limpa relacionado aos processos de produtos sustentáveis. O uso de combustíveis fósseis, principalmente no setor de transporte, é a principal fonte de emissão de gases do efeito estufa responsável pelas mudanças climáticas (CABRERA-JIMÉNEZ et al., 2022). Neste contexto, o uso de biocombustíveis líquidos pode facilitar, de maneira mais sustentável, a redução das emissões de carbono na atmosfera.

Um dos biocombustíveis mais comuns é o biodiesel, obtido em escala industrial, principalmente, via reação de transesterificação de óleos vegetais, gordura animal ou algas com um álcool de cadeia curta como, por exemplo, metanol ou etanol (GERPEN, 2005). Essa reação pode ser catalisada por álcalis, ácidos ou enzimas (SOKAČ et al., 2020). Atualmente, o processo químico convencional (catálise alcalina) representa a principal rota de produção industrial de biodiesel devido ao bom rendimento global obtido. No entanto, a principal desvantagem deste processo é a necessidade de matéria-prima refinada com baixo teor de ácidos graxos livres (AGL). Esse pré-refino pode representar cerca de 60-80% dos custos totais de produção de biodiesel (SANDOUQA; AL-HAMAMRE, 2021). Por essa razão, a produção de biodiesel mediada pelo uso de enzimas (lipases) tem recebido grande atenção especialmente por permitir o uso de óleos de baixo custo e de baixa qualidade, com alto teor de ácidos graxos livres (AGL), como matéria-prima, reduzindo assim o custo total de produção de biodiesel (LV et al., 2021). Ao final da reação de transesterificação, seja alcalina, ácida ou enzimática, tem-se a formação de impurezas como sabão, ácido graxo não reagido, álcool residual, água, glicerol livre, catalisador, mono- di- e triacilgliceróis que devem ser removidas. No entanto, as impurezas da reação enzimática são mais difíceis de serem removidas devido à baixa qualidade da matéria-prima utilizada. Dessa forma, um desafio do processo enzimático de produção



de biodiesel é conduzir a um produto final que atenta aos padrões de comercialização (LV et al., 2021).

Neste contexto, o desenvolvimento de tecnologias com intuito de otimizar o processo de produção biocatalítica do biodiesel faz-se necessário. Dentre as tecnologias disponíveis, o uso de membranas para promover um polimento do biodiesel vem sendo amplamente explorado como uma alternativa promissora para diminuir custos no processo de produção, fornecendo um combustível de alta qualidade além de baixo uso de energia, condições de temperatura e pressão moderadas, eliminação de tratamento de águas residuais, estabilidade mecânica, térmica e química (SOKAČ et al., 2020).

Portanto, o presente trabalho investiga o uso de membranas poliméricas comerciais na separação de contaminantes solubilizados visando o polimento dos ésteres metílicos de ácidos graxos. O desempenho da membrana na permeação de uma mistura bruta real obtida em um processo enzimático industrial é avaliado usando o modo de filtração de fluxo cruzado. Os parâmetros de fluxo de permeado da membrana, eficiência de separação e permeabilidade ao ar, água e biodiesel foram avaliados separadamente para membranas na forma de discos planos com diferentes características de hidrofiliicidade, hidrofobicidade e porosidade. Esta dissertação busca contribuir para estudos envolvendo o uso de membranas poliméricas comercialmente disponíveis para polimento de misturas de ésteres de ácidos graxos.

## **Objetivos**

Este trabalho propõe o estudo do polimento de ésteres metílicos de ácidos graxos (FAME) bruto real obtido por processo enzimático em escala industrial utilizando membranas poliméricas comerciais. Para isso, realizou-se (1) uma pré-seleção de membranas disponíveis comercialmente que foram utilizadas na (2) caracterização fluidodinâmica individualizada com ar, água e biodiesel “on spec” e (3) avaliação do desempenho das membranas selecionada no polimento de amostras industriais de FAME enzimático.

## Metodologia

Como método de execução da pesquisa, primeiramente, realizou-se uma busca por membranas poliméricas comercialmente disponíveis. Para isso, contatou-se várias empresas fornecedoras com intuito de promover a aquisição dessas membranas. Seis membranas com diferentes características e polaridades foram selecionadas e utilizadas na pesquisa, entre elas, poliamida (90 Da, 245 Da e 200 Da), fluoreto de polivinilideno (0.2  $\mu\text{m}$ ), politetrafluoretileno (0.05  $\mu\text{m}$ ) e polietersulfona (10 kDa). Todas as membranas adquiridas foram no formato de folha plana. Sequencialmente, foram obtidas duas amostras de ésteres metílicos de ácidos graxos obtidos via rota enzimática fornecidas por indústria parceira em colaboração com o projeto. Para os testes em laboratório, realizou-se a caracterização fluidodinâmica das membranas para estudo do escoamento ao ar, água e biodiesel “on spec”. Os ensaios para avaliar a permeabilidade ao ar foram realizados em regime permanente com fluxo de ar seco em temperatura ambiente (25 °C). A folha de membrana plana foi cortada em formato circular e selada com anéis de borracha dentro de uma porta amostras (cilíndrico) que proporcionou um diâmetro médio de 1,94 cm e uma área de 2,96 cm<sup>2</sup>. A queda de pressão através da membrana foi medida por meio de um manômetro em função da variação do fluxo de ar, e posteriormente calculou-se a velocidade superficial do fluido. Os ensaios de permeabilidade à água e ao biodiesel foram realizados no mesmo aparelho de laboratório e sob as mesmas condições (regime permanente com fluxo de água e biodiesel “on spec” em temperatura ambiente). As amostras de membranas foram cortadas e seladas com anéis de borracha dentro de um porta-amostras cilíndrico fornecendo um diâmetro útil de 10,2 cm e uma área de 81,7 cm<sup>2</sup>. Água e biodiesel “on spec” foram bombeados através da membrana em sistema de fluxo cruzado sob um gradiente de pressão fixo em 3 bar. Com isso, foi medida a massa permeada em função do tempo com uma proveta graduada, para, posteriormente, se calcular a vazão volumétrica e velocidade superficial do líquido. Para os ensaios de desempenho de filtração da membrana, o mesmo aparelho foi utilizado. As amostras de membranas foram primeiramente pré-condicionadas em biodiesel “on spec” em módulo de filtração de fluxo cruzado a 3 bar por um período de 6 h. Após o condicionamento, a mesma membrana era submetida à filtração com as

amostras reais de ésteres metílicos de ácidos graxos industriais obtidos via rota enzimática. Calculou-se o fluxo de permeado e parâmetros de permeabilidade. O permeado coletado foi enviado à indústria parceira para realização das análises quantitativas. As amostras de permeados foram analisadas quantitativamente em termos de sabão, acidez, umidade, cor e contaminação total seguindo métodos padronizados ASTM D664 e ASTM D1796.

## **Resultados e Discussão**

As duas amostras de ésteres metílicos de ácidos graxos obtidos via rota enzimática foram caracterizadas quantitativamente em termos de sabão, acidez, umidade e densidade. Comparou-se o comportamento de permeabilidade ao fluxo de fluido gasoso (ar) e de fluidos líquidos (água e biodiesel “on spec”). Observou-se que os valores de permeabilidade ao ar foram maiores quando comparados ao fluxo de líquido devido à tensão superficial que dificulta o escoamento (permeação) pelos poros da membrana, promovendo uma resistência. As amostras de FAME industrial bruto foram filtrados em um processo de fluxo cruzado à temperatura ambiente e gradiente de pressão de 3 bar. Com base no fluxo de permeado e na análise quantitativa do conteúdo nos permeados, o desempenho das membranas foi avaliado. Os resultados mostraram que apenas a membrana de ultrafiltração de polietersulfona (PES) com limite de peso molecular (MWCO) de 10 kDa apresentou potencial para polimento de biodiesel. A membrana de polietersulfona apresentou o melhor desempenho, reduzindo totalmente o teor de sabão no permeado, além da cor, contaminação total e teor de fósforo das amostras. Os teores de acidez e água também foram reduzidos de acordo com a análise quantitativa, porém em menores proporções. Não houve permeação com as membranas de nanofiltração de poliamida. Por outro lado, para a membrana de microfiltração (PVDF) observou-se total permeação das amostras de ésteres metílicos de ácidos graxos não sendo eficiente no processo de separação das impurezas contidas nas amostras de FAME industrial.

## **Conclusão**

O objetivo geral de polimento de amostras reais industriais de ésteres de ácidos graxos enzimático foi alcançado. Observou-se que a membrana de polietersulfona 10 kDa foi capaz de remover 100% do sabão em todos os testes de filtração, e levar a excelentes níveis de cor dentro do padrão de cor da escala Gardner. Além disso, a permeação através dessa membrana baixou os níveis totais de contaminação e fósforo com valores obtidos até 0,58 mg/kg e 0,51 mg/kg, respectivamente, atendendo as especificações padrão estabelecidas pela ASTM. Embora a concentração final de água (o menor valor obtido foi de 893 ppm) e acidez (o menor valor obtido foi de 1,56%) ainda não atendam às especificações da norma ASTM (menos de 200 ppm para água e menos de 0,50% para acidez), o uso da membrana de polietersulfona de ultrafiltração 10kDa é uma alternativa adequada para polimento de mistura de ésteres metílicos de ácidos graxos. Portanto, o processo de separação por membranas é uma alternativa adequada para o polimento FAME, reduzindo o número de etapas a jusante do processo.

## ABSTRACT

Enzymatic biodiesel processes have attracted great interest in industrial production. The greatest advantage of the enzymatic process, when compared to the conventional chemical process, is that it can use low-quality and cheap feedstock with high free fatty acid (FFA) and water contents. Moreover, enzymatic processes present mild reaction conditions, low energy consumption, easy product recovery, and thus are environmentally friendly and low-cost processes. Nevertheless, a major challenge for the enzymatic process is to separate various impurities such as soap, fatty acid unreacted, residual alcohol, water, free glycerol, catalyst, phosphorus, sulfur, mono-, di-, and triglycerides that are formed after esterification and transesterification reaction due to low-quality feedstock to produce a final biodiesel product that meets the standards. Based on this, steps of biodiesel polishing are required to remove impurities. In this work, we propose the application of the membrane separation process to polishing crude industrial enzymatic fatty acid methyl esters (FAME). Six different membranes, polyamide (NF90, NF245, NF8038), Polyvinylidene fluoride (PVDF), Polytetrafluoroethylene (PTFE), and Polyethersulfone (PES) were selected and used for FAME filtration. Crude industrial FAME was filtrated in a crossflow process at room temperature and 3 bar transmembrane pressure. Permeance parameters for the flow of air, water, and “on spec” biodiesel were evaluated separately for membranes. Based on permeate flux and quantitative content analysis in the permeates, membrane performance was evaluated. The obtained results showed that the 10 kDa PES membrane had the best performance resulting in the exemption of soap content in permeate. Moreover, the PES membrane was successfully able to reduce the color, total contamination, and phosphorus content of FAME samples. Acidity and water content were also reduced. Therefore, the membrane separation process is a suitable alternative for FAME polishing, reducing the number of downstream steps.

**Keywords:** Membrane. Separation Process. Fatty acid methyl esters. Polishing. Biodiesel.

## LIST OF FIGURES

<b>Figure 1.</b> Schematic representation of the transesterification reaction. ....	21
<b>Figure 2.</b> Schematic representation of flowchart conventional biodiesel production. ....	23
<b>Figure 3.</b> Decision tree for selection of separation technology. ....	28
<b>Figure 4.</b> Biodiesel produced via enzymatic processing. ....	30
<b>Figure 5.</b> Filtration spectrum of reverse osmosis, nanofiltration, ultrafiltration, microfiltration, and particulate filtration relative to the pore size. ....	32
<b>Figure 6.</b> Schematic flowchart of the methodology employed.....	39
<b>Figure 7.</b> Pictures of the tested membranes: a) NF90; b) NF8038; c) NF245; d) PES; e) PTFE; f) PVDF. ....	40
<b>Figure 8.</b> Useful filtration diameter represented on the membrane surface. ....	45
<b>Figure 9.</b> Schematic view of FAME flow permeation apparatus.....	46
<b>Figure 10.</b> Front view of bench equipment used for liquid tests as well as system components.....	46
<b>Figure 11.</b> Experimental device in: (a) "on spec" biodiesel permeation tests and (b) real industrial enzymatic fatty acid methyl esters sample tests. ....	48
<b>Figure 12.</b> Experimental air and water permeation curves for all membranes of different pore sizes. ....	52
<b>Figure 13.</b> Water flux experimental for micro-and nanofiltration membranes. ....	53
<b>Figure 14.</b> Drop test to determine hydrophobic or hydrophilic membrane character. ....	54
<b>Figure 15.</b> "On spec" biodiesel used in permeation assays. ....	55
<b>Figure 16.</b> Permeate flux (a) and permeance (b) NF90 membrane (90 Da) with "on spec" biodiesel after 360 min of permeation under TMP = 3 bar. The permeate points were collected after 34 min of operation.....	56
<b>Figure 17.</b> Permeate flux (a) and permeance (b) NF245 membrane (245 Da) with "on spec" biodiesel after 360 min of permeation under TMP = 3 bar. The permeate points were collected after 120 min of operation.....	57
<b>Figure 18.</b> Permeate flux (a) and permeance (b) NF8038 membrane (200 Da) with "on spec" biodiesel after 360 min of permeation under TMP = 3 bar. The permeate points were collected after 120 min of operation.....	58
<b>Figure 19.</b> Membrane surface after permeation tests with "on spec" biodiesel: (a) NF245 and (b) NF-90. ....	60

<b>Figure 20.</b> Permeate flux (a) and permeance (b) PVDF membrane (0.2 $\mu\text{m}$ ) with “on spec” biodiesel after 120 min of permeation under TMP = 3 bar. The permeate points were collected immediately after the start of the operation. ....	61
<b>Figure 21.</b> PVDF Membrane surface after permeation tests with “on spec” biodiesel. ....	62
<b>Figure 22.</b> Permeate flux (a) and permeance (b) PES membrane (10 kDa) with “on spec” biodiesel during 360 min permeation under TMP = 3 bar (conditioning for the first filtration test with industrial FAME). The permeate points were collected 120 min of operation. ....	63
<b>Figure 23.</b> Permeate flux (a) and permeance (b) PES membrane (10 kDa) with “on spec” biodiesel during 360 min permeation under TMP = 3 bar (conditioning for the second filtration test with industrial FAME). The permeate points were collected after 120 min of operation.....	64
<b>Figure 24.</b> Permeate flux (a) and permeance (b) PES membrane (10 kDa) with “on spec” biodiesel during 360 min permeation under TMP = 3 bar (conditioning for the third filtration test with industrial FAME). The permeate points were collected after 120 min of operation.....	65
<b>Figure 25.</b> Dry membrane module after filtration test.....	67
<b>Figure 26.</b> Surface NF-90 membrane after contact with industrial FAME in separation attempt. ....	67
<b>Figure 27.</b> PVDF Membrane surface after permeation tests with industrial FAME. ..	68
<b>Figure 28.</b> Permeate flux (a) and permeance (b) PES membrane with industrial FAME (sample 467) after 280 min of permeation under TMP = 3 bar.....	69
<b>Figure 29.</b> Schematic representation of the steps for obtaining permeates. ....	70
<b>Figure 30.</b> Membrane surface after direct contact with real industrial FAME for 280 min in a crossflow filtration system at 3 bar.....	72
<b>Figure 31.</b> Permeate flux (a) and permeance (b) 10 kDa PES membrane with industrial FAME (sample 467) after 12 h of permeation under TMP = 3 bar.....	73
<b>Figure 32.</b> Membrane surface after direct contact with real industrial FAME for 12 h in a crossflow permeation system at 3 bar. ....	74
<b>Figure 33.</b> Permeates obtained during 12 h of filtration. ....	74
<b>Figure 34.</b> Schematic representation of the steps for obtaining permeates from the Erechim sample. ....	76

<b>Figure 35.</b> Permeate flux (a) and permeance (b) PES membrane with industrial FAME (sample Erechim) after 70 h of permeation under TMP = 3 bar. ....	77
<b>Figure 36.</b> Membrane surface after direct contact with real industrial FAME for 70 h in a crossflow filtration system at 3 bar. ....	78
<b>Figure 37.</b> Quality Permeates obtained by ultrafiltration polyethersulfone. Feed and concentrate (retained) are represented by O and C, respectively. ....	80
<b>Figure 38.</b> Fatty acid methyl ester obtained after polishing through UF with 10 kDa PES membrane. ....	80



## LIST OF TABLES

<b>Table 1.</b> Current Brazilian biodiesel standards.....	26
<b>Table 2.</b> Works using membranes in biodiesel polishing/purification. ....	36
<b>Table 3.</b> Technical information of the commercial polymeric membranes used in the search. ....	43
<b>Table 4.</b> Composition and properties of the fatty acid methyl ester (FAME) mixtures used in the tests. ....	50
<b>Tabela 5.</b> Average values of air and water permeance for membrane tested. ....	52
<b>Table 6.</b> Soap, acidity, and moisture content after ultrafiltration with polyethersulfone membrane. ....	71
<b>Table 7.</b> Soap, acidity, moisture content, and color after ultrafiltration with the 10 kDa PES membrane. ....	75
<b>Table 8.</b> Soap, phosphorus, acidity, moisture content, color, and total contamination after UF with 10 kDa PES membrane. ....	78

## LIST OF ABBREVIATIONS AND ACRONYMS

ABNT	Associação Brasileira de Normas Técnicas
ANP	National Agency of Petroleum, Natural Gas and Biofuels
ASTM	American Society for Testing and Materials
DG	Diglycerides
FAAE	Fatty Acid Alkyl Esters
FAEE	Fatty Acid Ethyl Esters
FAME	Fatty Acid Methyl Esters
FFA	Free Fatty Acids
HP	Heavy Phase
HVO	Hydrotreated Vegetable Oil
J	Permeate Flux
LP	Light Phase
MG	Monoglycerides
MWCO	Molecular Weight Cut-Off
P	Permeance
PDMS	Polydimethylsiloxane
PES	Polyethersulfone
PTFE	Polytetrafluoroethylene
PSf	Polysulfone
PVDF	Polyvinylidene Fluoride
TG	Triglycerides
TMP	Transmembrane Pressure
Vs	Surface Fluid Velocity

## SUMMARY

<b>1 INTRODUCTION</b> .....	<b>20</b>
<b>2 OBJECTIVES</b> .....	<b>22</b>
2.1 GENERAL OBJECTIVES .....	22
2.2 SPECIFIC OBJECTIVES.....	22
<b>3 LITERATURE REVIEW</b> .....	<b>20</b>
3.1 BIODIESEL SYNTHESIS AND PRODUCTION.....	20
3.2 FUEL STANDARDS FOR BIODIESEL.....	25
3.3 BIODIESEL POLISHING .....	27
<b>4 MATERIALS AND METHODS</b> .....	<b>39</b>
4.1 MEMBRANES .....	39
4.2 INDUSTRIAL FATTY ACID METHYL ESTER MIXTURE .....	43
4.3 PERMEANCE MEASUREMENT .....	43
4.4 FATTY ACID METHYL ESTERS FILTRATION ASSAYS IN A CROSSFLOW SYSTEM.....	45
4.4.1 Permeate flux .....	48
4.4.2 Permeance .....	49
4.5 PERMEATE QUALITY ANALYSIS.....	49
<b>5 RESULTS AND DISCUSSION</b> .....	<b>50</b>
5.1 INDUSTRIAL FATTY ACID METHYL ESTER MIXTURE QUANTIFICATION.....	50
5.2 AIR AND WATER PERMEANCE .....	51
5.3 “ON SPEC” BIODIESEL PERMEANCE ASSAYS .....	54
5.4 FILTRATION PERFORMANCE FOR FAME POLISHING USING POLYMERIC MEMBRANE.....	66
<b>6 CONCLUSIONS AND PERSPECTIVES</b> .....	<b>81</b>
REFERENCES.....	82

## 1 INTRODUCTION

Biofuels are liquid fuels produced, directly or indirectly, from renewable biomass matter (biological raw material) such as plants, animal fats, or microorganisms (ROBERTS; PATTERSON, 2014; RUAN et al., 2019). The concept of biofuels emerges as an effective solution to the impending global crisis in the current scramble to face up peak oil demand. These environmentally friendly fuels present several advantages over fossil fuels, such as reducing greenhouse gas emissions, i.e., low carbon dioxide, nitrogen oxide, and sulfur oxide emissions into the atmosphere, as well as biodegradability (RUAN et al., 2019). Out of a variety of fields of renewable energy sources such as solar, wind, biomass, and hydroelectric power, biofuels represent the major share of the current global energy demand, mainly in the transportation sector (MA et al., 2018; SUBRAMANIAM; MASRON; AZMAN, 2020; YANG et al., 2021). According to the International Energy Agency (IEA, 2020), the global production of transport biofuel in 2021 could have reached 162 billion liters, from which ethanol makes up 67% (~109 billion liters), biodiesel corresponds to 26% (~43 billion liters) and HVO (Hydrotreated Vegetable Oil) accounts for the remaining 7% (~10 billion liters) (IAE, 2020). In this scenario, biodiesel has attracted considerable interest as an alternative biofuel to replacing petrodiesel on a global scale (DOS SANTOS et al., 2017; LV; SUN; LIU, 2019).

Biodiesel is one of the most used biofuels since it can be pumped, stored, and handled using the same infrastructure employed for conventional diesel fuel (LUKOVIC; KNEEVIC-JUGOVIC; BEZBRADIC, 2011). Also, biodiesel has shown similar physicochemical properties to those of diesel, i.e., produces comparable power performance when burned in diesel engines (HASSAN; KALAM, 2013; LUKOVIC; KNEEVIC-JUGOVIC; BEZBRADIC, 2011; PRICE et al., 2016; SOKAČ et al., 2020). Biodiesel chemical structure is defined as Fatty Acid Alkyl Esters (FAAE) derived from sustainable feedstock, such as vegetable and algae oils or animal fats (BHARATHIRAJA et al., 2014; DUBÉ; TREMBLAY; LIU, 2007; KRISHNASAMY; BUKKARAPU, 2021; MOHIDDIN et al., 2021). In general, transesterification reaction is the most commercially favorable method for biodiesel production in the presence of short-chain alcohols (methanol and ethanol) and a catalyst, such as alkalis, acids, or enzymes (LAM; LEE; MOHAMED, 2010; LEUNG; WU; LEUNG, 2010).

However, the feasibility of the use of transesterification in industrial processes depends on important variables: alcohol to oil molar ratio (excess alcohol is normally used), temperature, pressure, and feedstock quality (GOMES; ARROYO; PEREIRA, 2011). Another issue is that after transesterification, the final mixture comprises alkyl esters of fatty acids, glycerol, residual alcohol, soap, water, catalyst, and mono-, di- and triglycerides (BHARATHIRAJA et al., 2014; BUDŽAKI et al., 2020; GOMES; ARROYO; PEREIRA, 2011). Therefore, these impurities must be removed from the biodiesel phase to meet the standard specifications based on ASTM D6571 or EN14214 so that, finally, biodiesel reaches the market (KNOTHE, 2005).

Purification of biodiesel is an expensive step that can be accomplished using various separation techniques. These processes are estimated to account for approximately 60-80% of the total cost of biodiesel production (SUTHAR; DWIVEDI; JOSHIPURA, 2019).

Several techniques have been tested for biodiesel purification, based on equilibrium-based, affinity-based, and membrane-based separation processes (BATENI; SARAEIAN; ABLE, 2017). The selection of an adequate separation technique is a crucial step in the purification process, according to the mixture of chemical species to be treated. The most frequently used method for biodiesel purification is liquid-liquid extraction, also known as wet washing (SOKAČ et al., 2020). However, it has some limitations such as the generation of a large volume of wastewater, high demand for energy, and low economic efficiency (SOKAČ et al., 2020). In this context, many studies have been carried out using membrane technology to reduce water consumption during the biodiesel purification step, and consequently decrease the process costs. Membrane filtration has been suggested as an environmentally friendly method and provides high-quality fuel. Other positive issues are the low usage of energy, moderate temperature and pressure conditions, and higher mechanical, thermal, and chemical stability of the separation devices (SOKAČ et al., 2020).

Membrane technology is very versatile in biodiesel purification and it can be applied to separate different species of the solution governed by two selectivity principles: size exclusion and affinity mechanism (ATADASHI; AROUA; AZIZ, 2011). In addition, membrane separation can be attached to reactors and allows continuous operation, i.e. a selective mass transport takes place with simultaneous reaction to

remove specific components from the reaction mixture (DUBÉ; TREMBLAY; LIU, 2007; MULINARI; OLIVEIRA; HOTZA, 2020). Membranes can be employed for the separation of glycerol (ALVES et al., 2013; SALEH; TREMBLAY; DUBÉ, 2010), as well as residual catalysts (ATADASHI et al., 2014), mono-, di-, and triglycerides (TAJZIEHCHI; SADRAMELI, 2021), and soap (WANG et al., 2009). Padula *et al.* (2022) applied modified membranes in the dehydration of fatty acid ester mixtures and the results showed an outstanding performance, which makes this technology very promising for implementation in the industrial sector.

The present work investigates the purification (also known as polishing) of biodiesel using commercial polymeric membranes for the separation of contaminants solubilized in biodiesel. The membrane performance in the permeation of a real crude mixture obtained in an industrial enzymatic process was evaluated using crossflow filtration mode. Membrane permeate flux, separation efficiency, and permeance parameters for the flow of air, water, and biodiesel were evaluated separately for membranes in the form of flat discs with different hydrophilicity/hydrophobicity characteristics and cut diameters. Thus, this dissertation seeks to contribute to studies involving the use of commercially available polymeric membranes for polishing fatty acid ester mixtures.

## **2 OBJECTIVES**

### **2.1 GENERAL OBJECTIVES**

This work studies the purification of real crude FAME obtained in an industrial enzymatic process using commercial polymeric membranes.

### **2.2 SPECIFIC OBJECTIVES**

- Pre-selection of commercially available membranes;
- Individualized fluid dynamic membrane characterization with air, water, and biodiesel;
- Performance evaluation of selected membranes in the polishing of industrial enzymatic FAME samples.

### 3 LITERATURE REVIEW

This chapter presents the theoretical background and a literature review with emphasis on membrane separation processes for biodiesel purification.

#### 3.1 BIODIESEL SYNTHESIS AND PRODUCTION

Biodiesel is one of the most used biofuels to supply the energy demand of the world due to its high biodegradability, low gaseous emissions, and chemical composition that results in comparable power performance with diesel when burned in engines. Thus, it can be used either on its own or mixed with conventional diesel fuel in existing diesel engines (NATH et al., 2020; NEJAD; ZAHEDI, 2018; TOPARE et al., 2021). Biodiesel (monoalkyl esters of fatty acids from vegetable oils and animal fats) can be produced by many processes, such as pyrolysis, microemulsions, and transesterification (LUKOVIC; KNEEVIC-JUGOVIC; BEZBRADIC, 2011). Pyrolysis employs a variety of thermal energy provided to chemical change (thermal decomposition) of triglycerides for the production of alkanes, alkenes, alkadienes, aromatics, and carboxylic acid. Pyrolyzed vegetable oils generally present a higher cetane number and lower viscosity when compared to pure vegetable oils (YADAV et al., 2019). However, they have some limitations that may hinder their biodiesel production implementation, such as the removal of oxygen as a function of thermal treatment, which eliminates the environmental advantages of using an oxygenated fuel (YADAV et al., 2019). Although microemulsions have been suggested as an option for decreasing the viscosity of vegetable oils, fuel produced by this method spawn engine performance problems (ATADASHI et al., 2014; YADAV et al., 2019).

Among processes for biodiesel synthesis, transesterification has many advantages to produce good quality and environmentally friendly fuel from vegetable oils. Transesterification (alcoholysis) is the most common method for converting triglycerides and short-chain alcohols (methanol or ethanol) to biodiesel, i.e., is a process similar to hydrolysis where takes place the displacement of alcohol from an ester by another, the big difference is that it uses alcohol instead of water (MEHER; VIDYASAGAR; NAIK, 2006). The characteristics of biodiesel by this process are, among several others, high cetane number and low flashpoint (LUKOVIC; KNEEVIC-

JUGOVIC; BEZBRADIC, 2011). Figure 1 shows a general schematic representation of the transesterification reaction.

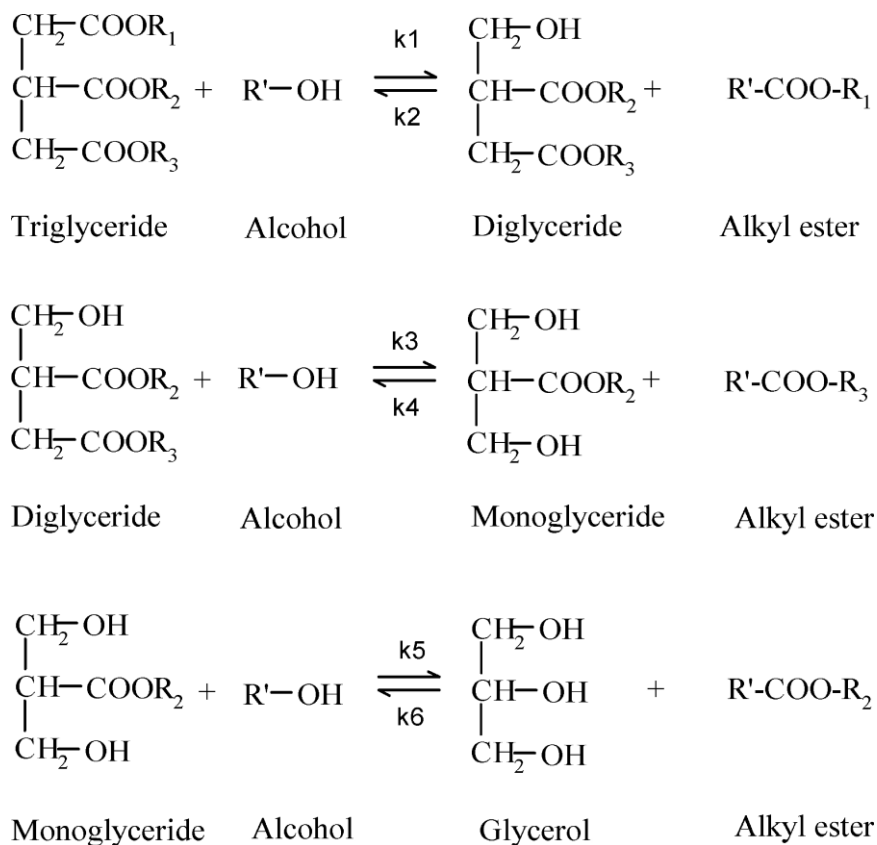


**Figure 1.** Schematic representation of the transesterification reaction.

Source: (CAO et al., 2007).

In Figure 1, long-chain hydrocarbon (or fatty acid chain) such as palmitic acid,  $(\text{CH}_2)_{14}\text{-CH}_3$  are represented by  $\text{R}_1$ ,  $\text{R}_2$ , and  $\text{R}_3$ . Radical  $\text{R}'$  corresponds to alcohol used for the production of biodiesel, usually methanol or ethanol. The transesterification process is a reversible reaction that takes place by a three-step mechanism. Firstly, triglycerides are converted into diglycerides. The latter, in turn, are converted into monoglycerides, and then finally into methyl or ethyl ester of fatty acids and glycerol as the main byproduct (CAO et al., 2007).

The use of catalysts in reaction for biodiesel production can be advantageous since accelerates the conversion. Transesterification is enhanced by three types of catalysts: acid, base, or enzymatic (MOHIDDIN et al., 2021). Acid or base catalysts can be classified into two main categories: heterogeneous and homogeneous. A heterogeneous catalyst forms two or more phases (nonuniform) with other reactants.



The components separate and the composition varies and can be separated through physical processes, e.g., filtration or centrifugation. In a homogeneous catalyst, the reaction constituent phases are uniform in appearance and can only be separated by adding or creating another phase within the system. Biodiesel production needs a stable catalyst that can be easily separated from the reaction media and reused several times. This feature makes heterogeneous catalysts advantageous. Nevertheless, the reaction rate of heterogeneously catalyzed transesterification is lower when compared to the homogeneously catalyzed reaction (MOHIDDIN et al., 2021).

In terms of biodiesel industrial processing, alkali catalyzed transesterification is the most widely used due to the high reaction rate. Common basic catalysts used are sodium hydroxide, potassium hydroxide, sodium methoxide, and potassium methoxide (THANGARAJ et al., 2019). Base-catalyzed transesterification can keep its high performance. However, it produces soap in the presence of free fatty acids (FFA) and water that can solidify at room temperature and reduce production yield. To overcome these drawbacks, acid homogeneous catalysts can be used, such as sulfuric acid (THANGARAJ et al., 2019). An acid pre-treatment process is usually necessary to reduce the FFA content to a level below 1% (MARDHIAH et al., 2017). This pre-treatment has several drawbacks as increased process costs, the need for high-quality feedstocks (low free fatty acid and water contents), high energy consumption, and difficult glycerol recovery (GOG et al., 2012; LV et al., 2017). Figure 2 shows a process flowchart of biodiesel production.

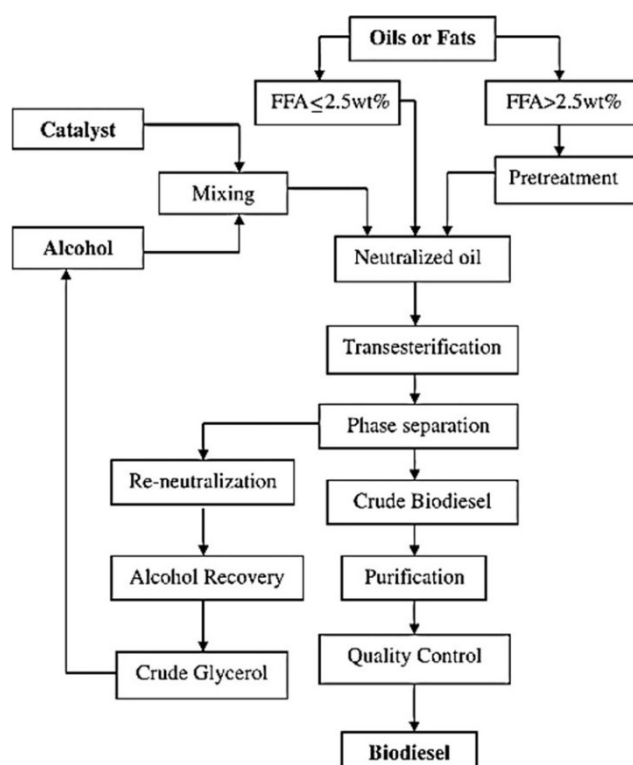


**Figure 2.** Schematic representation of flowchart conventional biodiesel production.

Source: (MARDHIAH et al., 2017).

The use of refined oils as feedstock accounts for approximately 80% of total biodiesel production costs (COSTA et al., 2020). For this reason, the use of low-cost feedstock for biodiesel production makes the process economically attractive. Nevertheless, unrefined oil has high free fatty acid (FFA) and water contents, not recommended for use directly in the alkali-catalyzed transesterification reaction. As shown in Figure 2, pretreatment of this oil is required to avoid the aforementioned problems and the increased biodiesel production costs. In this scenario, hydroesterification becomes a promising alternative because it allows to produce high-quality biodiesel, and there is no need for pretreating the feedstock. Overall, hydroesterification is a hydrolysis reaction followed by an esterification reaction. Firstly, all unrefined oil is hydrolyzed thus forming FFA and glycerol. Subsequently, the hydrolysis reaction occurs, where FFAs are esterified with an alcohol (usually methanol or ethanol) to produce biodiesel and water (COSTA et al., 2020; MANDOLESI DE ARAÚJO et al., 2013). Water-soluble glycerin is the main side product of triglyceride hydrolysis reaction and the consequence is a two-phase system with a heavy phase

(HP) consisting of water, glycerin, and alcohol, and a light phase (LP) consisting of glycerides, FFA, and FAME. Biodiesel is commonly produced via hydroesterification by using lipases as catalysts.

Lipases (triacylglycerol hydrolases, EC 3.1.1.3) are the most used enzymes as biocatalysts for hydroesterification or transesterification reactions due to tolerance to organic solvents and thermal stability (MULINARI; OLIVEIRA; HOTZA, 2020). Therefore, biocatalytic processes have received significant attention and development. Enzymatic hydro/transesterification presents several advantages over chemical transesterification in industrial processes such as high selectivity, high specificity, high conversions of free fatty acids under mild environmental conditions, good quality of final product, and decreased generation of wastewater (NORJANNAH et al., 2016). The main advantage of biological catalysts is to enable the use of low-grade, low-cost raw materials (unrefined), i.e., remove additional pre-treatment steps reducing the global production costs (MIBIELLI et al., 2019; REMONATTO et al., 2016). It is worth mentioning that, despite the large variety of feedstock qualities available, a simple and robust pretreatment process will ensure an efficient enzymatic reaction. The main point is to neutralize the mineral acidity, as it lowers the pH of the water-glycerin-alcohol phase (heavy phase) and this promotes enzyme inactivation. This explains why the FFA acidity does not adversely affect the enzyme, as FFA is dissolved in the oil phase (The Novozymes Enzymatic Biodiesel Handbook, [s.d.]).

Most feedstocks suitable for the enzymatic biodiesel process vary in composition, quality, and physical appearance. The major disadvantage is that the final biodiesel product contains more impurities that are difficult to remove when compared to biodiesel produced from the refined and uncontaminated feedstock. Thus, separation technologies that allow the refining of biodiesel produced via the enzymatic hydroesterification route are needed. The separation techniques will be briefly discussed in Section 3.3, focusing on studies involving the use of membrane technology for biodiesel purification.

The feasibility of the use of enzymes in industrial processes depends on several factors: reaction temperature, water amount in the system, alcohol-to-oil ratio, and alcohol type. The reaction temperature can vary depending on enzyme activity or stability. For instance, when *T. lanuginosa* is used for catalyzing transesterification (using methanol) of sunflower oil, the optimal temperature is 50 °C. On the other hand,

in the same reaction, the optimal temperature for *R. miehei* is 40 °C or lower. It is important to take into account the water content in the system because enzymes are sensitive to water and need a small amount of water for activation. On the other hand, increasing water content promotes a favorable effect to reverse reaction (hydrolysis) and the catalytic activity can decrease (LUKOVIC; KNEEVIC-JUGOVIC; BEZBRADIC, 2011; MARDHIAH et al., 2017).

### 3.2 FUEL STANDARDS FOR BIODIESEL

Biodiesel fuels must meet ASTM (American Society for Testing and Materials) Standard Specification that is made to evaluate the characteristics as well as provide the specification for the biodiesel presents appropriate values for different chemical and physical properties (SINGH et al., 2019). The main parameter reported that significantly affects the value of the characteristics of biodiesel is the feedstock quality (in terms of water content, free fatty acid, and saturation level). Several of the main physicochemical properties are described in ASTM D6751, EN 14214, and ISO 15607 standards for biodiesel (SINGH et al., 2019).

Quality standards for biodiesel, intended for marketing, are based on a variety of factors according to the characteristics of each region, e.g., diesel fuel standards for that region, types of diesel most common in the region, climatic properties, and type of feedstock available of the region or country where it is produced. In Europe, the main feedstocks used for biodiesel production are sunflower and rapeseed oil, unlike USA and Canada, which use soybean and waste vegetable oil. Because of this, there is not a universal quality specification of biodiesel (MONTERO, 2011).

In Brazil, biodiesel specifications are established by the National Agency of Petroleum, Natural Gas and Biofuels (ANP), and the quality standards were constituted based on ASTM D6751 and EN 14214 (LÔBO; FERREIRA; CRUZ, 2009). These standards are suitable for both FAME (fatty acid methyl ester) and FAEE (fatty acid ethyl esters) (MONTERO, 2011). The fuel standards for biodiesel are shown in Table 1.

**Table 1.** Current Brazilian biodiesel standards.

<b>Biodiesel B-100</b>		
<b>Parameters</b>	<b>Unit</b>	<b>Especificacion</b>
Aspect	-	LII <sup>(1)</sup>
Specific Gravity (20 °C)	kg/m <sup>3</sup>	850.0 a 900.0
Kinematic Viscosity (40 °C)	mm <sup>2</sup> /s	3.000 a 6.000
Water Content <sup>(2)</sup>	mg/kg	Max. 200
Methanol Content	% m/m	Max. 0.20
Total Contamination	mg/kg	Max. 24.0
Flash Point	°C	Min. 100.0
Ester Content	% m/m	Min. 96.5
Sulfated Ash	% m/m	Max. 0.02
Total Sulfur	mg/kg	Max. 10.0
Sodium (Na) and Potassium (K)	mg/kg	Max. 5.0
Calcium (Ca) and Magnesium (Mg)	mg/kg	Max. 5.0
Phosphorus (P)	mg/kg	Max. 10.0
Copper Corrosion (3 h at 50 °C)	-	Max. 1.0
CFPP <sup>(3)</sup>	°C	Max. 14.0
Acid Number	mg KOH/g	Max. 0.50
Free Glycerin	% m/m	Max. 0.020
Total Glycerin	% m/m	Max. 0.250
Monoglycerides	% m/m	Max. 0.700
Diglycerides	% m/m	Max. 0.200
Triglycerides	% m/m	Max. 0.200
Iodine Number	g I <sub>2</sub> /100g	Note
Oxidation Stability (110°C)	h	Min. 12
Cetane Number	-	Note

(1) Clear and free of impurities, indicating the test temperature. In case of dispute, the product can only be considered as not specified in the aspect if the parameters of water content and/or total contamination are non-compliant.

(2) For inspection purposes, in the fines for non-compliance, a variation of +50 mg/kg in the water content limit in biodiesel will be allowed for the producer and +150 mg/kg for the distributor.

(3) The limit depends on each state. For the states not included by the standard, the cold fouling point will remain at 19 °C.

Source: ("Resolução ANP N° 45 DE 25/08/2014", 2014)

Several points and criteria allow the grouping of the main properties of biodiesel. Among the most important are: engine properties, such as fuel-air mixture combustion, exhaust gas quality, and ignition condition. Moreover, cold weather properties, which comprise cold point and pour point as well as transport, deposition, and engine parts

properties, e.g., oxidation stability, flash point, microbial contamination, and viscosity are part of the main properties of biodiesel (MONTERO, 2011).

### *3.3 BIODIESEL POLISHING*

Crude fatty acid esters must be treated in the polishing step after the transesterification reaction. Besides fatty acid esters, the mixture still contains impurities such as unreacted free fatty acids, soap, free glycerol, excess alcohol, water, trace of residual catalyst, mono-, di-, and triglycerides (MOAZENI; CHEN; ZHANG, 2019). The selection of an adequate separation technique is a crucial step in biodiesel polishing. The purification process should be selected according to the mixture of chemical species to be treated.

Most separation technology knowledge can be organized into a query system for an approach to the selection and sequencing of adequate methods for separating multicomponent liquid mixtures, as summarized in Figure 3. In general, this method approaches the division of a complex problem into simpler subproblems eliminating unfeasible alternatives. This approach eventually decreases operation costs in chemical process industries (DIMIAN; BILDEA, 2008).

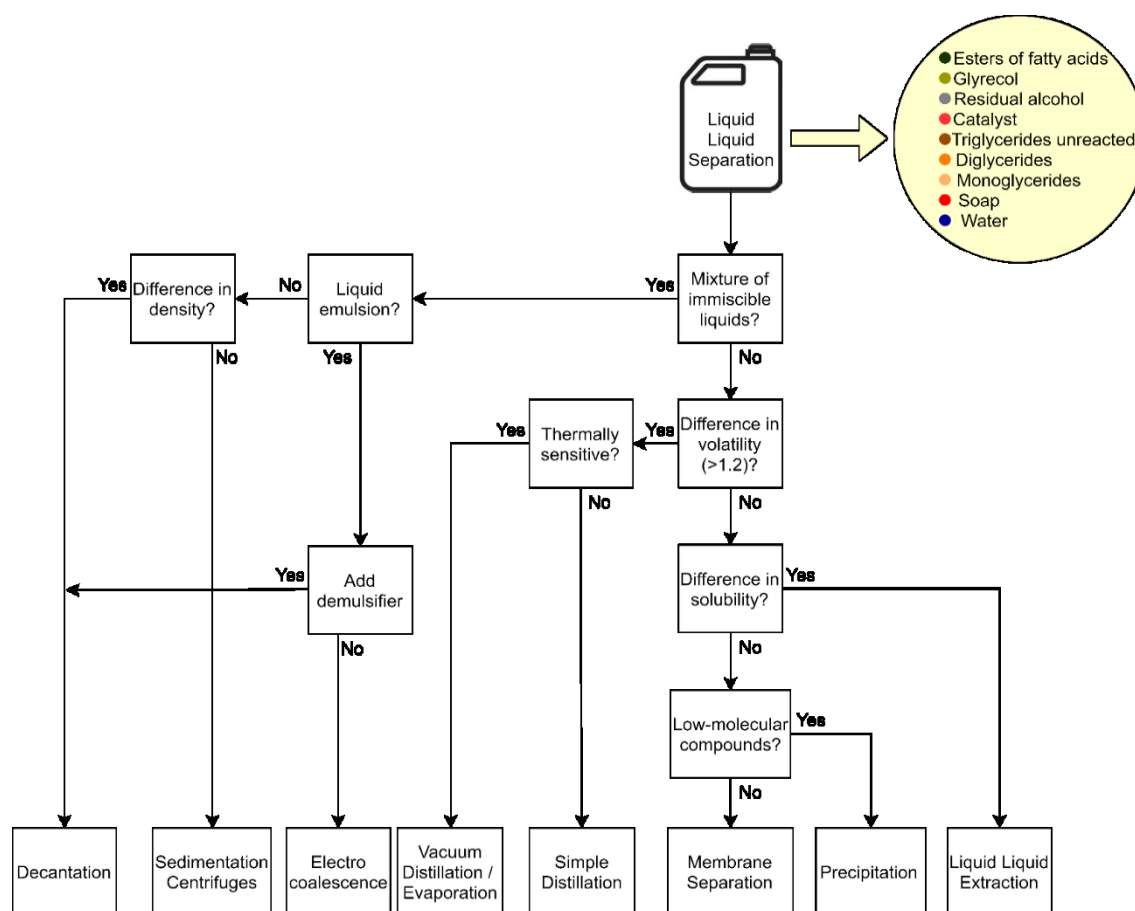


**Figure 3.** Decision tree for selection of separation technology.

Source: Author, 2022.

The separation techniques mainly seek to produce successfully the desired products with suitable purity. For the separation of a multicomponent liquid mixture, specific techniques or methods are needed for each case. In broad terms, given an n-component liquid mixture such as biodiesel, it is important to know the physicochemical properties of the mixture as the separation technique fundamental principle, whether physical or chemical, is to use the properties of the mixture components to separate them (BARNICKI; FAIR, 1990). These properties can be a melting point, boiling point, solubility, and density, among others.

For the separation of ester and glycerol phases, decantation or centrifuges are techniques most commonly used due to differences in the density of such compounds. Biodiesel and glycerol densities are  $880 \text{ kg/m}^3$  and  $1050 \text{ kg/m}^3$ , respectively (ATADASHI; AROUA; AZIZ, 2011). However, decantation has low efficiency with FAME-water emulsions containing small FAME droplets e.g., a long time is required

for complete separation of the FAME phase from the emulsions. For this case, the use of centrifuges becomes an alternative; however, there is a need for initial capital and periodic maintenance (SALEH; TREMBLAY; DUBÉ, 2010).

Distillation and evaporation techniques are generally described as a method to remove excess alcohol and water from crude biodiesel (ATADASHI et al., 2011). Nevertheless, distillation or even vacuum distillation for separation of FAME from heavy compounds such as triglycerides (TG), diglycerides (DG), and monoglycerides (MG) does not overcome the glycerol purity issue, since some glycerol is transported during the distillation process (SALEH; TREMBLAY; DUBÉ, 2010). Among the possible well-established large-scale separation techniques, liquid-liquid extraction (LLE) is the most common method used in biodiesel polishing. LLE with deionized water is applied to remove soap, residual catalyst, and remaining alcohol.

The procedure is usually very simple: water is used to extract the desirable compounds from biodiesel by mass transfer, taking two primary factors into account: water temperature and volume. For example, glycerol flows more easily from biodiesel to water at a higher temperature due to lower viscosity and higher glycerol diffusivity. In addition, the more water used, the higher the mass transfer area, so the higher the volumetric mass transfer coefficient. After the wet washing technique, the biodiesel needs to be dehydrated to an acceptable content according to ASTM standards. A timely separation technique refers to electro-coalescence. The main drawback of wet washing is high energy consumption and the use of a large amount of water generating wastewater (ATADASHI et al., 2011).

Biodiesel produced via enzymatic processing requires unique polishing methods. In biodiesel plants, filtration is the most common polishing method for the separation of, for example, sterol glucosides and other impurities that can be easily filtered out. Nevertheless, the filtration process represents an important step in biodiesel processing and must, therefore, always be improved. Recently, membrane filtration methods have been studied. The type of polishing method that is needed for a particular plant will depend on the plant's design and which fuel standard it is aiming to meet ("Polishing perspectives: new biodiesel production technologies are likely to require different fuel polishing procedures", 2012). Figure 4 shows a flowchart of the enzymatic production of biodiesel via the methylic route, highlighting the filtration



stage, specifically the membrane filtration process. Membrane processes are of great interest because they reduce the number of downstream unit operations.

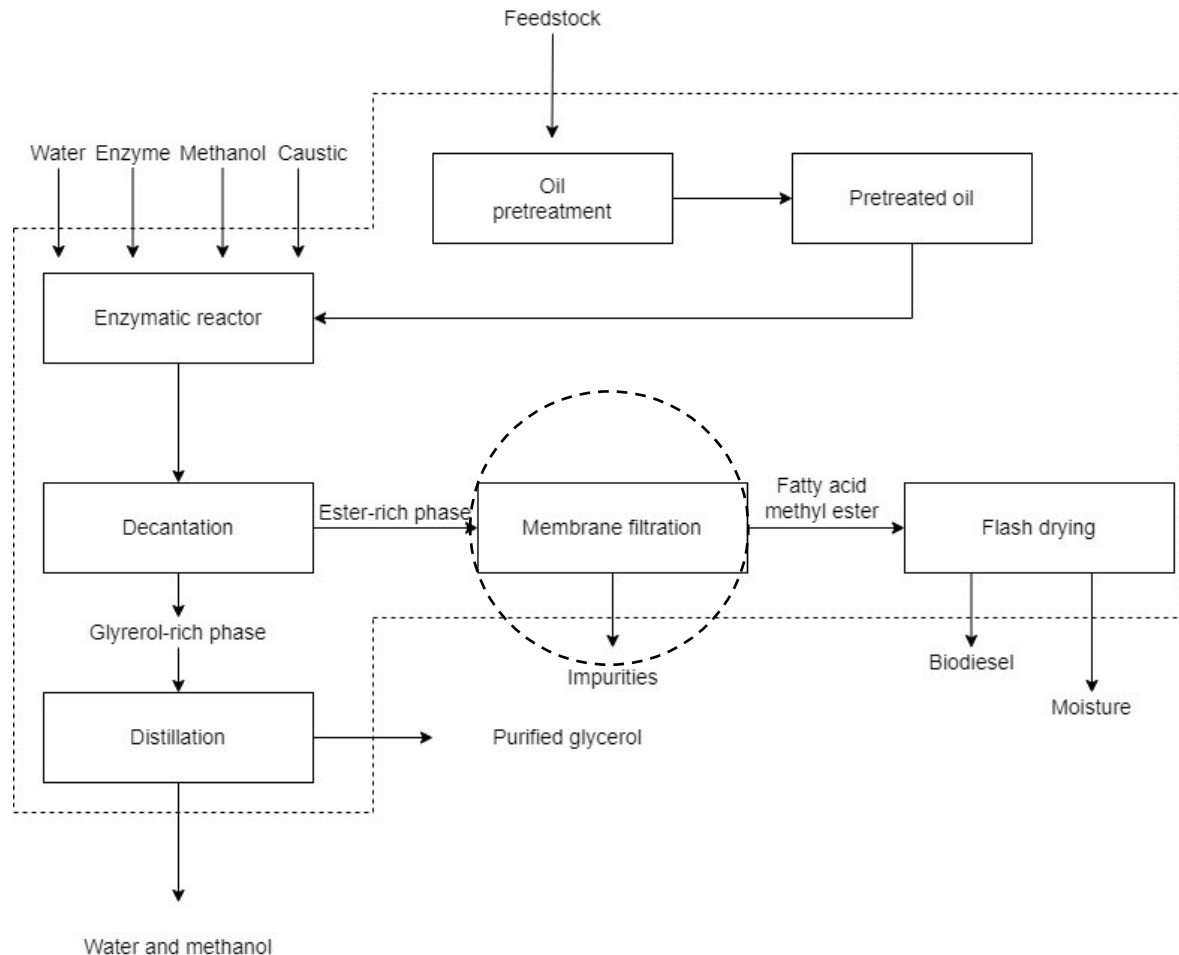


**Figure 4.** Biodiesel produced via enzymatic processing.

Source: Adapted from (The Novozymes Enzymatic Biodiesel Handbook, [s.d.]

Another strategy to enhance the efficiency of polishing crude biodiesel is to introduce membrane technology. Studies report a good performance process providing high-quality biodiesel (ALVES et al., 2013; ATADASHI et al., 2015). Membrane separation has been suggested as a low or no water alternative in the polishing of crude biodiesel (KRISHNASAMY; BUKKARAPU, 2021). Generally speaking, membranes are semipermeable barriers that are used in the selective separation of solubilized or suspended compounds in a fluid medium. Mass transfer through a membrane takes place by concentration, pressure, or temperature gradient. Membrane-based separation requires a suitable combination of membrane polarity

and molecular weight cut-off. Membrane separation technology has great potential to promote solutions to environmental problems such as valuable product recovery, and wastewater treatment as well as minimizing their harm to the atmosphere (SALEH; TREMBLAY; DUBÉ, 2010).

Membrane filtration can be classified depending on the pore size as conventional filtration (1 – 1000  $\mu\text{m}$ ), microfiltration (0.1 – 10  $\mu\text{m}$ ), ultrafiltration (10 – 50  $\mu\text{m}$ ), nanofiltration (1 – 5 nm), and reverse osmosis (nonporous). Figure 5 shows how membrane technology allows the separation of very small molecules, which dimensions can be measured in Angstrom. The characteristics of microfiltration membranes are usually expressed in terms of the micrometers ( $\mu\text{m}$ ), while the separation characteristics of nanofiltration and ultrafiltration membranes are typically expressed in terms of the molecular weight cut-off (MWCO, or more commonly as “Dalton”). Membrane manufacturers supply detailed information in terms of Dalton, for example, 200 Da or 10 kDa. Chemically, the Dalton unit of measurement is related to the molecular weight of the particle, e.g., a unit Dalton is equal to the molar mass of the particle expressed in grams per mol (1 Da = 1 g/mol). The major compounds in biodiesel are triacylglycerol (890 g/mol), diacylglycerol (624 g/mol), and monoacylglycerol (358 g/mol) followed by soap (306 g/mol), ester (299.54 g/mol), fatty acid (282.46 g/mol), glycerol (92.07 g/mol), catalyst: enzyme (19-60 g/mol) or alkali (40-56 g/mol), methanol (32.04 g/mol), and water (18.02 g/mol) (ULIANA et al., 2018). Thus, the choice of adequate pore size depends on the characteristics of the feedstock and the solution to be treated (JOSE; KAPPEN; ALAGAR, 2018).

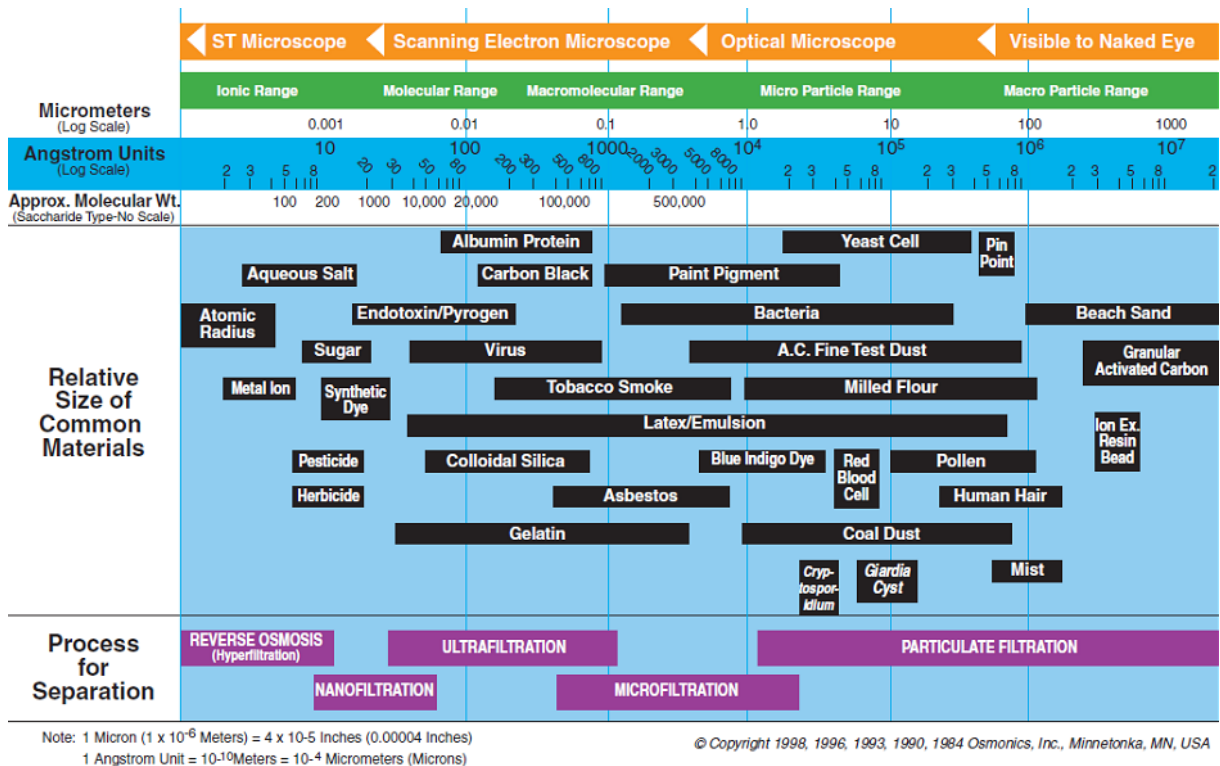


**Figure 5.** Filtration spectrum of reverse osmosis, nanofiltration, ultrafiltration, microfiltration, and particulate filtration relative to the pore size.

Source: (RADCLIFF; ZARNADZE, 2004)

Besides, membranes can also be divided into groups considering the producing materials, namely organic (polymers), and inorganic (ceramic or metals). Membrane fouling is the main drawback that causes flux decline over time due to solute adsorption on membrane and pore surfaces causing pore blockage. Fouling can be reversible or irreversible and cause an increase in TMP to maintain a specific flux, or a decrease in flux when the system is operated at constant pressure (GUO; NGO; LI, 2012). Reversible fouling occurs due to the concentration polarization and deposition of solutes on the membrane rejection surface. Reversible fouling can be restored by backwashing. Irreversible fouling occurs through chemisorption and pore plugging mechanisms. The loss of transmembrane flux cannot be recovered, i.e. the membranes must be replaced (GUO; NGO; LI, 2012). Then, the compounds typically present in an oil feedstock – soap, glycerol, alcohol, mono- di- and triglycerides – become an important parameter to evaluate in the filtration system.

Several polymeric membranes have been tested for biodiesel polishing and purification. Sokac *et al.* (2020) directly compared four polymeric membranes

(polyethersulfone, polyacrylonitrile, polypropylene, and regenerated cellulose) for glycerol removal in enzymatic biodiesel purification by ultrafiltration. Based on permeate flux and glycerol content in aliquots permeated, they showed that polyacrylonitrile (pore size 0.2  $\mu\text{m}$ ) and polyethersulfone (10 kDa) membranes were promising. Nevertheless, polyacrylonitrile membrane showed the best performance with ultrafiltration efficiency of 91.48% with the lowest free glycerol content in permeate of 0.006% (w/w).

Alves *et al.* (2013) compared the application of micro and ultrafiltration membranes for biodiesel purification. The authors achieved successful separation of glycerol from biodiesel using ultrafiltration polyethersulfone membrane (MWCO of 10 kDa) with glycerol content below 0.02% (w/w), meeting the international standards. However, the permeate of the microfiltration membrane did not meet the minimum level of free glycerol content. Other membranes have been studied recently for biodiesel purification, including surface-modified membranes. Padula *et al.* (2022) made a surface modification on polymeric hydrophilic poly(vinylidene difluoride) microfiltration membranes using silazane to render them hydrophobic for biodiesel dehydration. They succeeded to dehydrate biodiesel using a membrane process.

Recently, Torres *et al.* (2018) proposed the use of a polymeric nanofiltration composite membrane to remove glycerol and total glyceride traces from biodiesel. Poly(vinylidene difluoride) (PVDF) membranes were coated with polydimethylsiloxane (PDMS) to improve membrane properties such as high solvent resistance. Remarkable flux stability after more than 20 cycles of biodiesel permeation was reported, and a rejection of 70% for glycerol and 69% for total glycerides with a permeate flux of 7.4  $\text{L}\cdot\text{m}^{-2}\cdot\text{h}^{-1}$ . In another study, Torres *et al.* (2017) evaluated the removal of glycerol of biodiesel from semi-refined soybean oil using lab-made ultrafiltration polymeric membrane of poly(vinylidene difluoride) (PVDF) and polysulfone (PSf) as main materials. PVDF membrane performance was higher than PSf, yielding a glycerol rejection of 67% and 48%, respectively. A remarkable flux recovery after more than 45 cycles of biodiesel permeation was observed in the PVDF membrane, supposedly indicating high stability and low membrane fouling.

Among inorganic materials, ceramic membranes have many advantages such as high chemical, mechanical and thermal resistance. Some examples of ceramic membrane materials used are alumina, silica, zirconia, titania, and carbides, among

others (MULINARI; OLIVEIRA; HOTZA, 2020). Usually, they are made on a support structure made of alpha-alumina, titanium oxide, or zirconium oxide. Inorganic membranes, likewise in the study involving organic membranes, have been studied in the literature in pore sizes in the ultrafiltration to microfiltration range. With a 0.05  $\mu\text{m}$   $\text{Al}_2\text{O}_3/\text{TiO}_2$  membrane, Atadashi *et al.* (2015) successfully met ASTM standards for free glycerol and soap in the final biodiesel product. The best operating conditions obtained were a pressure gradient of 2 bar, a temperature of 40 °C with flow rate, and permeate flux of 105  $\text{L}\cdot\text{min}^{-1}$  and 22.17  $\text{kg}\cdot\text{m}^{-2}\cdot\text{h}^{-1}$ , respectively. Gomes *et al.* (2013) evaluated the influence of acidified water addition in the application of micro- and ultrafiltration tubular  $\alpha\text{-Al}_2\text{O}_3/\text{TiO}_2$  membrane with pores size and cut-off of 0.2, 0.1, 0.05  $\mu\text{m}$ , and 20 kDa to separate glycerol from biodiesel produced by ethyl transesterification of degummed soybean oil. The experimental results showed that the addition of 10% of acidified water was necessary to reduce free glycerol content (<0.02 wt%) for commercialization. The best performance was achieved using ultrafiltration membranes (0.05  $\mu\text{m}$  and 20 kDa) with permeate flux of  $\sim 60 \text{ kg}\cdot\text{h}^{-1}\cdot\text{m}^{-2}$  under 1 bar pressure.

In a study by Wang *et al.* (2009), the authors introduced the microfiltration ceramic membranes (pore sizes of 0.6, 0.2, and 0.1  $\mu\text{m}$ ) to refine the palm biodiesel and remove the residual free glycerol, soap, and metals. According to the research, the membrane with a pore size of 0.1  $\mu\text{m}$  was very suitable for this separation due to its high permeate flux of 300  $\text{L}\cdot\text{m}^{-2}\cdot\text{h}^{-1}$ . The values of free glycerol (<0.0108% wt.) and metals were lower than the EN 14538 specification. Based on the literature studies, Atadashi *et al.* (2012) applied a multi-channel tubular-type  $\text{Al}_2\text{O}_3/\text{TiO}_2$  membrane with a pore size of 0.02  $\mu\text{m}$  to reduce free glycerol and potassium level. Moreover, a surface response methodology was used for the optimization of process parameters. This work showed that the ceramic membrane was able to decrease free glycerol and potassium levels below ASTM standards specification under optimal conditions of 2 bar, temperature 40 °C, and permeate flux 9.08  $\text{kg}\cdot\text{m}^{-2}\cdot\text{h}^{-1}$  reaching values of 0.007 wt% and 0.297  $\text{mg}\cdot\text{L}^{-1}$ , respectively.

A non-conventional method that is worth mentioning is the integration of transesterification with membrane separation into a membrane reactor. This approach can overcome the problems of the traditional technique. Among the advantages, operational simplicity, flexibility, high selectivity and permeability, low consumption of

energy, reaction, and separation into a single process can be mentioned (ATADASHI; AROUA; AZIZ, 2011). Dubé *et al.* (2007) studied the application of the membrane reactor in the separation of unreacted vegetable oil from the fatty acid methyl esters (FAME) to produce high-quality biodiesel. They used a semi-batch two-phase carbon membrane reactor. The carbon film with a membrane pore size of 0.05  $\mu\text{m}$  was able to retain the transfer of triglycerides and non-reacting lipids to the product stream. The great benefit is a simplification of the downstream step purification of FAME. Cao *et al.* (2007) studied the influence of the membrane pore size on biodiesel production on the performance of a membrane reactor. Four different carbon membranes of pore sizes 0.05, 0.2, 0.5, and 1.4  $\mu\text{m}$  were tested. All membranes were able to retain canola oil in the reactor, indicating that the emulsified oil droplets were larger than the membrane pores. In addition, the conversion rate of raw oil was higher than 90% in this integrated system, with an initial methanol/oil volume ratio of 0.38. In another work from these authors, high-quality FAME production varying free fatty acid (FFA) content in a membrane reactor was investigated. The membrane employed in the reactor system was a ceramic membrane with 300 kDa MWCO and constructed of a titanium oxide support. The membrane reactor presented a good performance, yielding high-quality FAME. Varying FFA in feedstock influenced FAME quality. Nevertheless, the final product from each feedstock met the ASTM D6751 standard (CAO; DUBÉ; TREMBLAY, 2008).

Table 2 presents the papers found in the literature involving the use of membranes specifically in biodiesel polishing/purification.

Although the use of membranes for biodiesel polishing has grown over the last decade, most studies have focused on glycerol separation. In this study, the goal was biodiesel polishing in terms of soap, color, total contamination, sulfur, acidity, and moisture.

**Table 2.** Works using membranes in biodiesel polishing/purification.

<i>Membrane separation process</i>	<i>Membrane type</i>	<i>Poro size/MWCO</i>	<i>Results</i>	<i>References</i>
Ultrafiltration	Polypropylene Polyethersulfone Polyacrilonitrile Regenerated cellulose	0.2 µm 10 kDa 0.2 µm 1 kDa	Based on the obtained results it was shown that the polyacrilonitrile membrane is most efficiente for glycerol removal. Efficiency was around 91.48% with average free glycerol content in permeate of 0.006% (w/w).	SOKAČ et al., 2020
Microfiltration	Tubular module ceramic membrane ( $\alpha$ -Al <sub>2</sub> O <sub>3</sub> /TiO <sub>2</sub> )	0.2 µm	The use of microfiltration with ceramic membrane was efficient to remove glycerol from biodiesel and the permeates obtained for all conditions showed free glycerol values lower than 0.02% (w/w), maximum specification limit.	GOMES; ARROYO; PEREIRA, 2011
Microfiltration and Ultrafiltration	Mixed cellulose ester (MF) Mixed cellulose ester (MF) Poly(ethersulfone) (UF) Poly(ethersulfone) (UF)	0.22 µm 0.30 µm 10 kDa 30 kDa	Between the analyzed membranes, the glycerol content level ( less than 0.02 wt%) was achieved only with the membrane of 10 kDa. This membrane also presented a suitable permeate flux.	ALVES et al., 2013
Ultrafiltration	Multi-channel tubular-type Al <sub>2</sub> O <sub>3</sub> /TiO <sub>2</sub> ceramic membrane	0.05 µm	Ceramic membrane separation system was developed to simultaneously remove free glycerol and soap from crude biodiesel. The best retention coefficients (%R) for free glycerol and soap were 97.5% and 96.6% respectively.	ATADASHI et al., 2015

Ultrafiltration	Modified hydrophilic polyacrylonitrile (PAN) membrane	100 kDa	The addition of small amounts of water was found to improve the removal of glycerol from FAME, and a glycerol content as low as 0.013 mass %, well below the standard of 0.020 mass %, was achieved.	SALEH; DUBÉ; TREMBLAY, 2010
Ultrafiltration	Modified hydrophilic polyacrylonitrile (PAN) membrane	100 kDa	Results showed low concentrations of water had a considerable effect in removing glycerol from the FAME even at approx. 0.08 mass%. Was use 2.0 g of water per L of treated FAME (0.225 mass% water).	SALEH; TREMBLAY; DUBÉ, 2010
Ultrafiltration	Multi-channel tubular-type Al <sub>2</sub> O <sub>3</sub> /TiO <sub>2</sub> ceramic membrane	0.02 µm	A ceramic membrane was used to purify crude biodiesel considering simultaneous retention of glycerol and catalyst. The values of free glycerol (0.007wt%) and potassium (0.297 mg/L) were all below ASTM standard specification.	ATADASHI et al., 2012
Microfiltration and Ultrafiltration	Tubular module ceramic membrane (α-Al <sub>2</sub> O <sub>3</sub> /TiO <sub>2</sub> )	0.2 µm (MF) 0.1 µm (MF) 0.05 µm (UF) 20 kDa (UF)	The ultrafiltration membranes, 0.05 µm and 20kDa (1.0 bar) promoted permeate flux above 60kg/hm <sup>2</sup> and glycerol content in the permeate lower than 0.02%, being thus selected as the most appropriate for glycerol separation.	GOMES; ARROYO; PEREIRA, 2013
Ultrafiltration	Tubular module ceramic membrane (α-Al <sub>2</sub> O <sub>3</sub> /TiO <sub>2</sub> )	0.05 µm  20 kDa	The ultrafiltration was efficient in removing glycerol, since the highest glycerol content in the permeate was 0.013wt%. The experiments were varying the transmembrane pressure and the concentration of the feed mixture.	GOMES; ARROYO; PEREIRA, 2015



Microfiltration	Ceramic membrane tube	0.1 $\mu\text{m}$ 0.2 $\mu\text{m}$ 0.6 $\mu\text{m}$	Microfiltration by ceramic membranes to remove the residual soap and free glycerol. The residual free glycerol in the permeate was estimated by water extraction, its value was 0.0108 wt.% to pore size of 0.1 $\mu\text{m}$ .	WANG et al., 2009
Microfiltration	Tubular module ceramic membrane ( $\alpha\text{-Al}_2\text{O}_3/\text{TiO}_2$ )	0.2 $\mu\text{m}$ 0.4 $\mu\text{m}$ 0.8 $\mu\text{m}$	This study investigated the efficiency of microfiltration with ceramic membranes in the separation of biodiesel and glycerol. The best performance was obtained with the 0.2 $\mu\text{m}$ membrane and 2 bar transmembrane pressure.	GOMES; PEREIRA; BARROS, 2010
Microfiltration and Ultrafiltration	Ceramic membrane	0.2 $\mu\text{m}$ (MF) 0.05 $\mu\text{m}$ (UF)	Ceramic membranes in the ultrafiltration (0.05 $\mu\text{m}$ ) and microfiltration (0.2 $\mu\text{m}$ ) ranges were tested at three different operating temperatures: 0, 5 and 25 $^\circ\text{C}$ . All runs separated glycerol from the crude FAME.	SALEH; DUBÉ; TREMBLAY, 2011)
Ultrafiltration	Poly(-vinylidene fluoride) (PVDF)  Poly(sulfone) (PSf)	570 - 600 kDa  75 - 81 kDa	The PVDF membrane reached a glycerol rejection up to 67% (at 30 $^\circ\text{C}$ and 5 bar) from a biodiesel sample with 0.5 wt % of water added. Under the same operation conditions, the PSf membrane showed a lower separation performance, with glycerol rejection of 48%.	TORRES et al., 2017
Microfiltration	Poly(-vinylidene fluoride) (PVDF)	0.2 $\mu\text{m}$	Membrane separation processes combined with membrane surface modification are shown to be a promising alternative for dehydration of mixtures of fatty acid esters obtained via biocatalysis.	PADULA et al., 2022

## 4 MATERIALS AND METHODS

This chapter describes the materials, equipment, and methods used to carry out this work. Figure 6 briefly presents a flowchart with a summary of the methodology employed to meet the proposed objectives, involving the stages in the development of this design, from the initial selection membranes to the final results obtained.

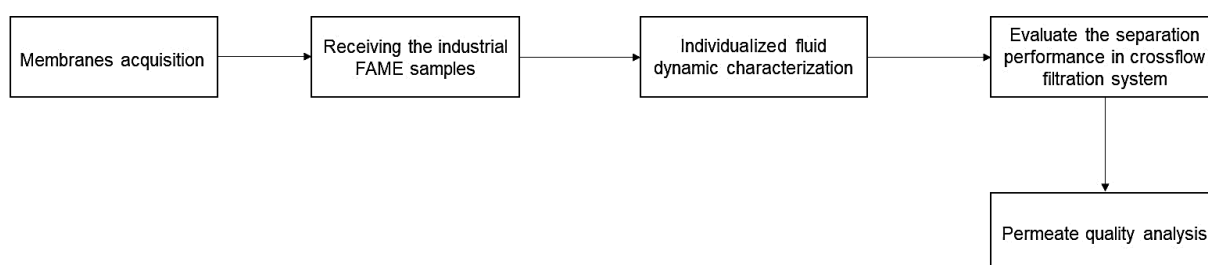


**Figure 6.** Schematic flowchart of the methodology employed

Source: Author, 2022.

### 4.1 MEMBRANES

The first stage of the work consisted of making a pre-selection of commercially available membranes. For this, membrane supply companies, which could support the project, were contacted. Two companies, Dupont and Koch Separation Solutions, have volunteered to donate available membrane samples, among them, nanofiltration (NF90, NF245, and NF) and ultrafiltration (PES) membranes. Initially, the criterion for the choice of membranes was mainly based on the molecular size of impurities in the fatty acid ester mixture. As discussed in Section 3.3, fatty acid esters are molecules smaller (292 to 298 Da) than soap and unreacted oils such as mono-, di-, and triglycerides (>298 Da). Therefore, membranes that could separate this molecular size range were sought.

The membranes were used as a porous separator for FAME impurities. The material used for membranes composition was polymeric (organic) due to its lower

cost and ease of element replacement. In this present search, a total of six different commercial polymeric membranes were tested and compared: three nanofiltration polyamide membranes (NF90, NF245, NF8038), one ultrafiltration polyethersulfone membrane (PES), and two microfiltration membranes of polyvinylidene fluoride (PVDF), polytetrafluoroethylene (PTFE). Figure 7 shows images of the flat sheet membranes. The membrane material and its characteristics, such as pore size are shown in Table 3.

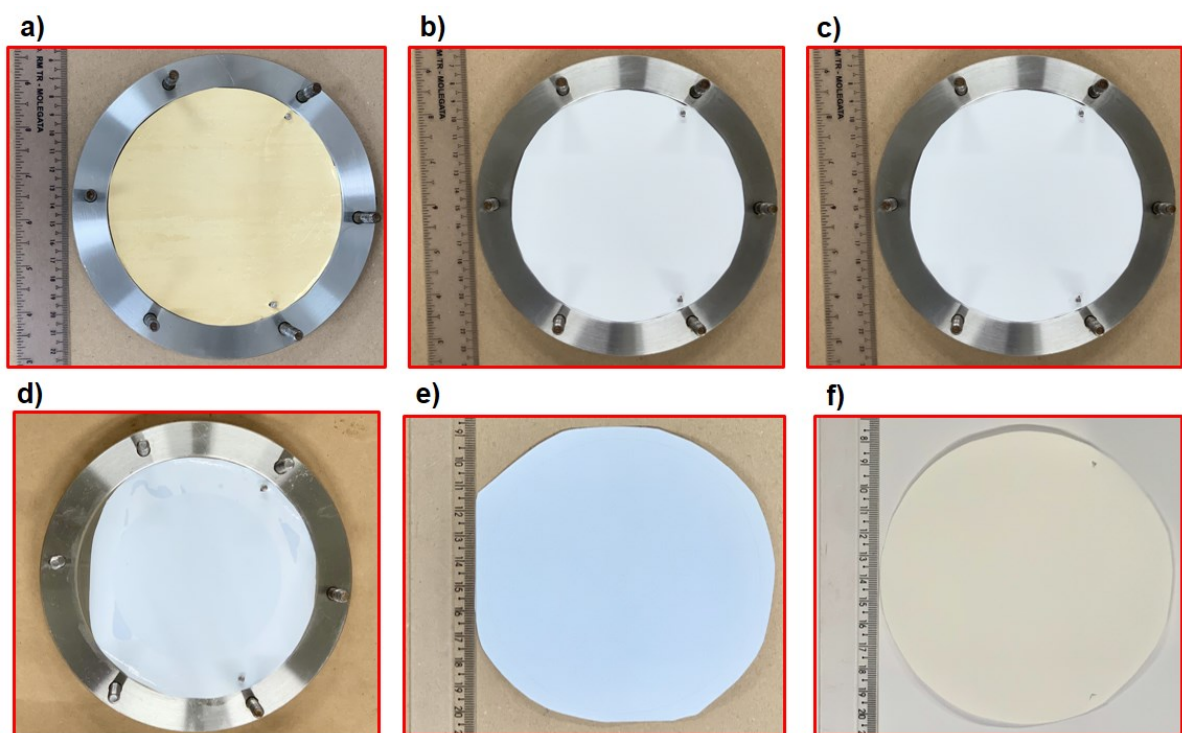


**Figure 7.** Pictures of the tested membranes: a) NF90; b) NF8038; c) NF245; d) PES; e) PTFE; f) PVDF.

Source: Author, 2022.

**Table 3.** Technical information of the commercial polymeric membranes used in the search.

Membrane	Type	Material	MWCO/Pore size	Process type	Supplier
NF 90	Flat sheets	Polyamide	90 Da	Nanofiltration	DuPont
NF8038	Flat sheets	Polyamide	200 Da	Nanofiltration	DuPont
NF 245	Flat sheets	Polyamide	245 Da	Nanofiltration	DuPont
PES	Flat sheets	Polyethersulfone	10 kDa	Ultrafiltration	Koch Separation
PTFE	Flat sheets	Polytetrafluoroethylene	0.05 $\mu\text{m}$	Ultrafiltration	Pall Coporation
PVDF	Flat sheets	Polyvinylidene fluoride	0.2 $\mu\text{m}$	Microfiltration	Microdyn - Nadir

\*Each membrane samples have a diameter of 10.2 cm and an active area of 81.7 cm<sup>2</sup>.

#### 4.2 INDUSTRIAL FATTY ACID METHYL ESTER MIXTURE

Different real fatty acid methyl ester samples were acquired from two partner companies (Prisma Brazil Group S.A, in Sumaré, SP, Brazil, and Olfar S.A, in Erechim, RS, Brazil). These real fatty acid methyl ester samples were collected from an industrial hydroesterification enzyme reactor plant, without purification step, and sent to the laboratory of the University of Ribeirão Preto (UNAERP). These samples were taken from a specific industrial batch of an enzymatic reactor and quantified in terms of acidity, moisture, soap, bound glycerin, and density. The second sample consists of “on spec” fatty acid methyl ester, i.e., this biodiesel sample meets the international specifications for commercialization. Real FAME samples were stored at room temperature (25 °C).

#### 4.3 PERMEANCE MEASUREMENT

Detailed comparative investigations are aimed in this study to reveal the air, water, and “on spec” biodiesel permeance behavior on the pore structures of available membranes. The permeance study allows for evaluating how easily a fluid can pass through the membrane pores. The permeance method was used to determine the flow rate by the pressure gradient, in a laboratory-made apparatus at UNAERP.

For measurements of air permeance, tests were carried out in a steady-state regime with dry airflow at room temperature (~25 °C). The membrane samples were sealed with rubber rings within a cylindrical stainless steel sample holder with a diameter of 1.94 cm and a flux area ( $A_{\text{flux}}$ ) of 2.96 cm<sup>2</sup>. The volumetric air flow rate was controlled by a needle valve and measured with a soap bubble flowmeter. The pressure drop was dependent on the variations in the air volumetric flow rate and was measured by a digital manometer. Flux rate ( $Q$ ) was corrected to the value at sample exit ( $Q_o$ ) and converted to superficial velocity by  $v_s = Q_o/A_{\text{flux}}$ . The collected data for each test was fit treated according to the least-square method using a parabolic model of the type:  $y = ax + bx^2$ , where  $y$  is  $\Delta P$  and  $x$  is the fluid velocity  $v_s$ . For the compressible flow of gases,  $\Delta P$  can be calculated by Equation 1 given by:

$$\Delta P = \frac{P_i^2 - P_o^2}{2P} \quad (1)$$

where  $P_i$  and  $P_o$  are, respectively, the absolute fluid pressures at the entrance and exit of the medium in kPa.  $P$  is the atmospheric pressure in kPa.

Experimental evaluation of water and “on spec” biodiesel permeance tests were carried out using laboratory equipment under the same conditions as air permeance tests. A cylindrical sample holder with a diameter of 10.2 cm and a circular flow area of 81.7 cm<sup>2</sup> was used in the assays. Figure 6 shows a sample of a flat sheet membrane inside the filtration module with the space limitation for the useful filtration diameter. Distilled water and “on spec” biodiesel were pumped through the membrane sample in a crossflow module. The pressure gradient across the sample was measured with a pressure transducer and can range from 0 – 10 bar. For permeance assays, the pressure gradient was fixed in 3 bar. In each experiment, water or “on spec” biodiesel mass flow rate through the membrane was obtained by mass (g) and time (s) measurements with a graduated tube. Enough time was waited to obtain a representative volume in the graduated tube to measure the corresponding mass, around 900 s (15 min).

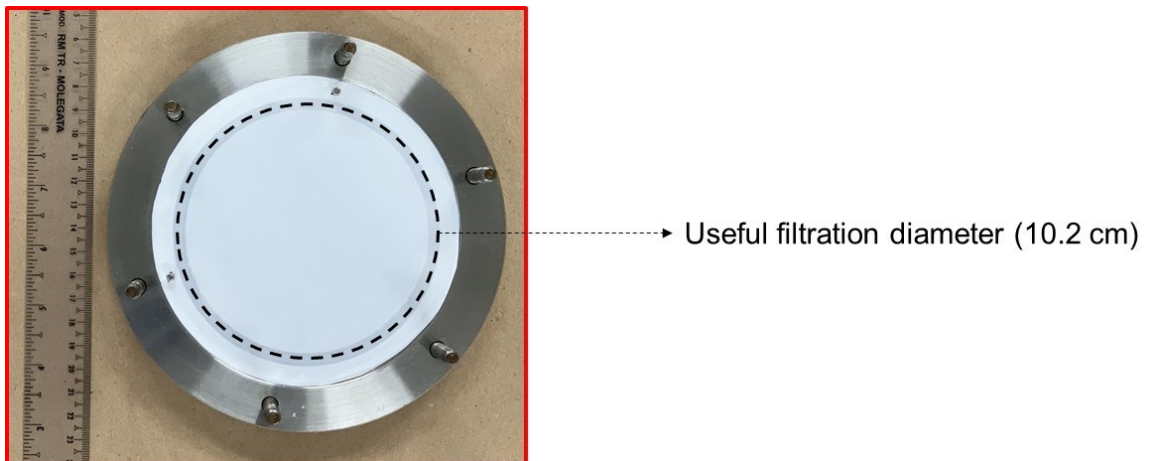


**Figure 8.** Useful filtration diameter (dotted lines) on the membrane surface.

Source: Author, 2022.

#### **4.4 FATTY ACID METHYL ESTERS FILTRATION ASSAYS IN A CROSSFLOW SYSTEM**

Similar to water and “on spec” biodiesel, filtration assays in a crossflow system were carried out. The system consisted of a feed tank, a positive displacement pump (Flojet, Bomsistema), a manometer, a valve, and a rotameter. The pumped liquid that reached the permeation module was divided into two streams, permeate and retentate, which both returned to the feed tank to maintain the feed concentration constant. A schematic diagram of the filtration plant is shown in Figure 9. The apparatus used for permeation tests is presented in Figure 10, indicating all system instruments.

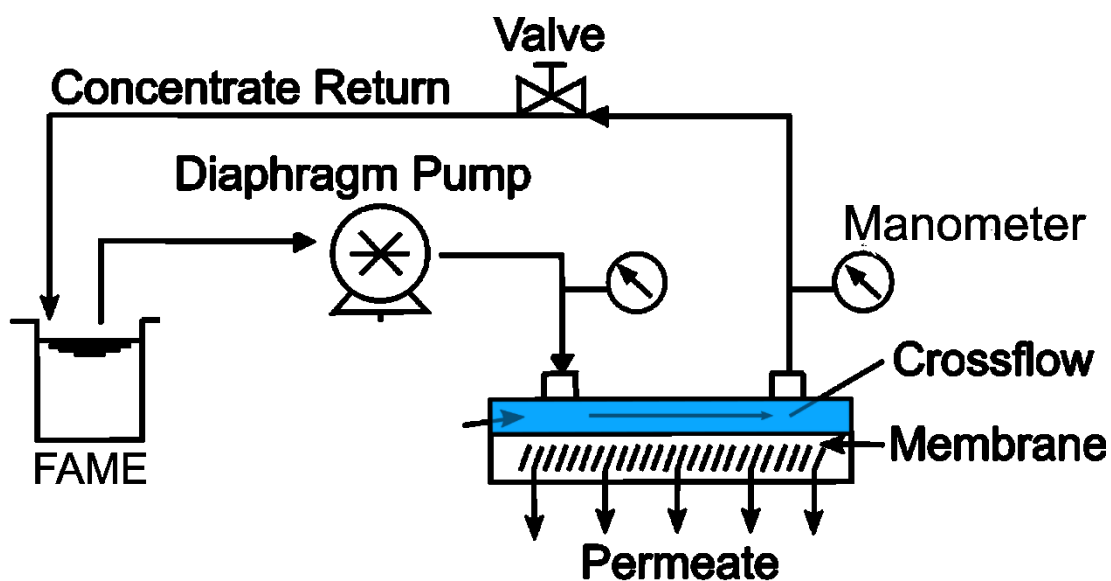


**Figure 9.** Schematic view of FAME flow permeation apparatus.

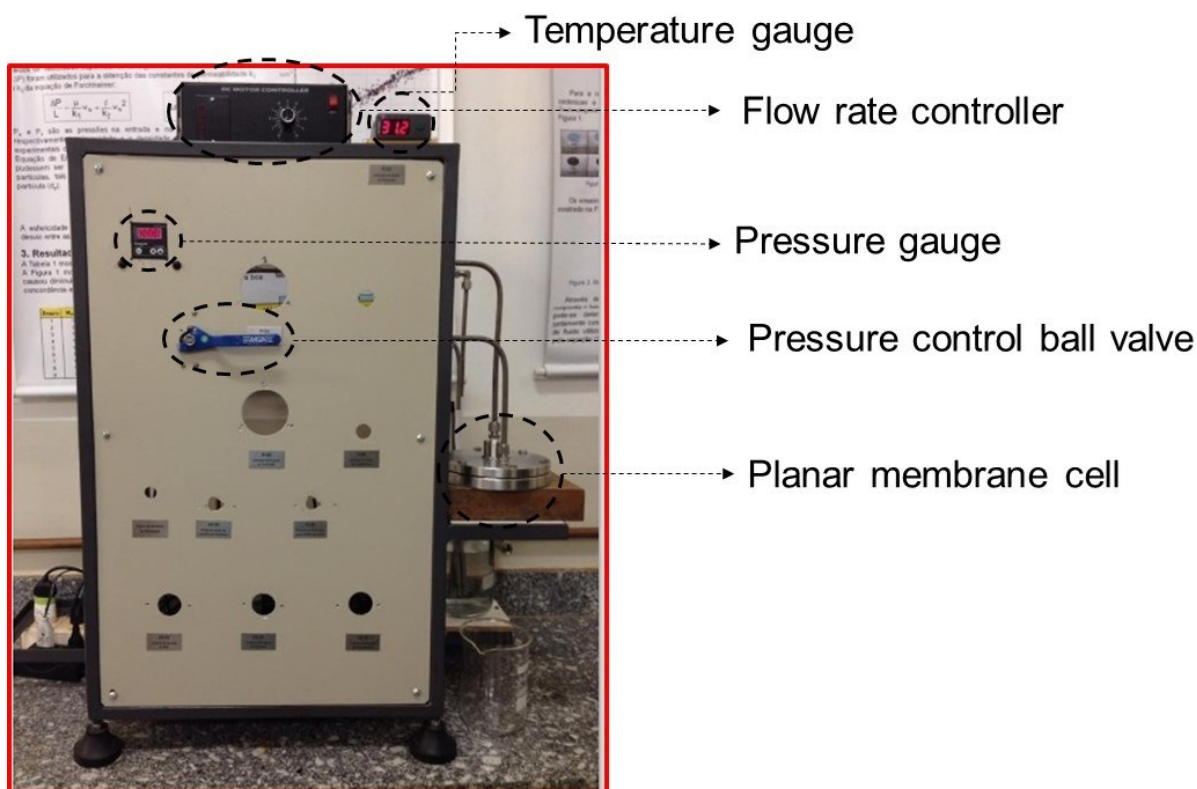


**Figure 10.** Front view of bench equipment used for liquid tests as well as system components.

Source: Author, 2022.

Six membranes were tested and compared. Before starting each permeation test with real crude FAME, the membranes were conditioned with “on spec” FAME (biodiesel) to evaluate permeate flux behavior (J) on membranes for FAME polishing. Before measurement of permeate flux, “on spec” biodiesel was passed in parallel to the membrane at pressure transmembrane (TMP) of 0 bar for 5 minutes to remove any contaminants from the membrane surface and the retentate was discarded. Then, the feed Erlenmeyer was filled with 400 mL of “on spec” biodiesel, and the permeate flux was measured at a TMP of 3 bar for 360 min. Aliquots of permeate were collected, and the flux was calculated each 15 min (time required to obtain a representative mass in the graduated tube). After membrane conditioning, a crude fatty acid methyl ester sample stored in a 1000 mL Erlenmeyer was pumped through the pre-conditioned membrane at room temperature (~25 °C) at least for 12 hours. The pressure gradient across the sample was measured with a pressure transducer and fixed in 3 bar, controlled by a ball valve, and the resulting biodiesel mass flow rate was obtained by mass (g) and time (s) measurements with a graduated tube. Sequentially, the FAME permeated volumetric flow rate was obtained by correlating it with FAME density, according to Equation 2.

$$Q = \frac{w}{\rho} \quad (2)$$

in which Q is the volumetric flow rate of permeated fluid (in m<sup>3</sup>/s or L/h), w is the mass flow rate of permeated fluid (in kg/s) and ρ is the FAME density (in kg/m<sup>3</sup> or kg/L). The density was measured employing a pycnometer.

Permeates collected during the recirculation of real FAME mixture in a crossflow system were stored for further quantitative analysis. Figure 11 illustrates the equipment in operation, Figure 11a with the “on spec” biodiesel sample, and Figure 11b with the real industrial enzymatic FAME.



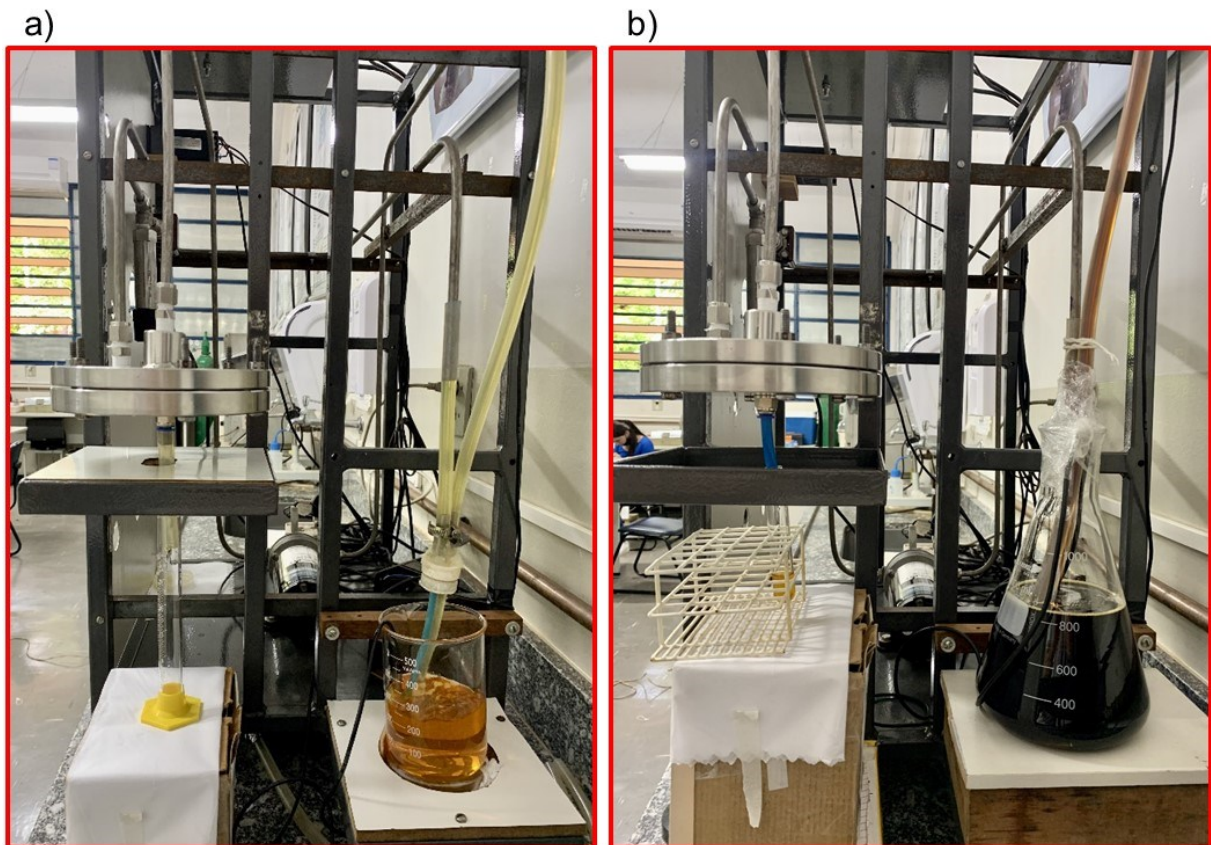


**Figure 11.** Experimental setup: (a) "on spec" biodiesel permeation tests and (b) real industrial enzymatic fatty acid methyl esters sample tests.

Source: Author, 2022.

It is worth mentioning that the central tube and the side tube correspond to the feed and the retained, respectively. A planar membrane cell is composed of a stainless steel piece that allows the tangential flow of the feed across the entire surface of the membrane making dragging easier and decreasing the fouling effects.

#### 4.4.1 Permeate flux

The flux ( $J$ ) of biodiesel permeated through the filtration membrane is given in  $L \cdot m^{-2} \cdot h^{-1}$  and can be obtained by:

$$J = \frac{M}{t \cdot \rho \cdot A_{flow}} \quad (3)$$

where  $A_{\text{flow}}$  is the superficial area of the medium exposed to flow ( $\text{m}^2$ ),  $M$  is the mass of biodiesel (kg) permeated in a given time  $t$  (s or h), and  $\rho$  is FAME density ( $\text{kg}/\text{m}^3$ ).

In summary,  $J$  can be obtained by the following relationship:

$$J = \frac{Q}{A_{\text{flow}}} \quad (4)$$

where  $Q$  is the volumetric flow rate of permeated FAME ( $\text{m}^3/\text{s}$  or  $\text{L}/\text{h}$ ) and  $A_{\text{flow}}$  is the superficial area of the medium exposed to flow ( $\text{m}^2$ ).

#### 4.4.2 Permeance

The membrane permeance ( $P$ ) can be obtained by:

$$P = \frac{J}{\Delta P} \quad (5)$$

where  $P$  is the membrane permeance ( $\text{L}\cdot\text{m}^{-2}\cdot\text{h}^{-1}\cdot\text{bar}^{-1}$ );  $\Delta P$  is the pressure gradient (bar); and  $J$  is the permeated flux ( $\text{L}\cdot\text{m}^{-2}\cdot\text{h}^{-1}$ ).

#### 4.5 PERMEATE QUALITY ANALYSIS

After collection, permeate samples were stored in test tubes (13 mL) with a cap to avoid any kind of external contamination. Thus, the permeate samples obtained were sent to permeate quality determination. Permeate samples were characterized in terms of soap, color, total contamination, acidity, and moisture, following ASTM D664, ASTM D6304, and EN 12662 standardized methods, and performed by a partner company (Prisma Brazil Group S.A).

## 5 RESULTS AND DISCUSSION

The present chapter discusses the results obtained from the polishing of enzymatic fatty acid ester samples on the polymeric membrane. First, different quantification values of the industrial enzymatic fatty acid methyl ester samples are presented. Then, permeance behavior to air, water, and “on spec” biodiesel is discussed. Finally, the membrane that showed the potential for biodiesel polishing and showed the best performance resulting in fatty acid methyl ester with better quantitative aspects will be further discussed.

### 5.1 INDUSTRIAL FATTY ACID METHYL ESTER MIXTURE QUANTIFICATION

In this investigation, a crossflow filtration system was used to test two feed mixtures with different compositions. The quantitative results of the samples used in the assays in terms of acidity, moisture, soaps, color, and density are shown in Table 4.

**Table 4.** Composition and properties of the fatty acid methyl ester (FAME) mixtures used in the tests.

<b>FAME Sample</b>	<b>Acidity (%)</b>	<b>Moisture (ppm)</b>	<b>Soaps (ppm)</b>	<b>Color <sup>a</sup> (gardner)</b>	<b>Density (g/cm<sup>3</sup>)</b>
467	4.54	7000	558	16.0	0.883
Erechim <sup>b</sup>	2.15	1018	449.5	12.8	0.884

<sup>a</sup> The Gardner color number is described in values 1-18, the proper standard for biodiesel is <10.

<sup>b</sup> Initial phosphorus content: 16.89 mg/kg.

Source: Author, 2022.

Moreover, it is important to take into account the fatty acid methyl ester feedstock. The FAME sample 467 was produced from Acid Sebum (GT, Bios, Caeté, MG) and the industrial FAME sample was produced from sludge cutting fatty acid (chemical refining) from Oleoplan, Veranópolis, RS.

## 5.2 AIR AND WATER PERMEANCE

The normalized pressure drop curves ( $\Delta P/L$ ) as a function of superficial fluid velocity ( $v_s$ ), for air or distilled water, were experimentally assessed for membranes with different pore sizes. Results are presented in Figure 12. Note that air permeance values are higher when compared with water flow due to surface tension present in liquids. This fact hinders the liquid permeation through membrane pores, causing further membrane resistance. The pressure drop varied with the features of the membrane, i.e., lower pore sizes and porosities provided a higher pressure drop as the membrane structure requires a greater driving force to promote air or water permeation.

Table 5 shows the average values of air and water permeance. As expected, microfiltration membranes such as PVDF (0.2  $\mu\text{m}$ ) exhibited permeance higher than those of ultra- or nanofiltration membranes like PTFE (0.05  $\mu\text{m}$ ) and NF245 (245 Da). If the goal of a project is to achieve high permeate rates, PVDF microfiltration membrane or even PTFE ultrafiltration membrane are possible alternatives. Nevertheless, there is a need to analyze them for their retention performance to promote adequate FAME polishing.

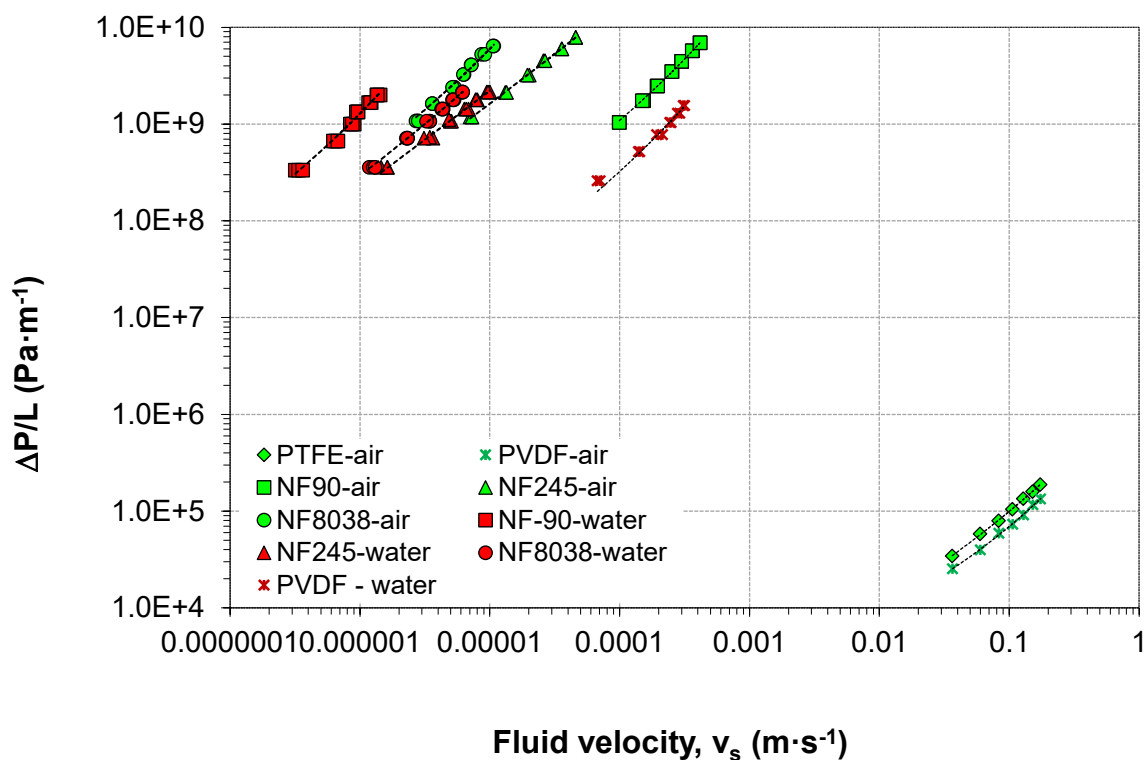


**Figure 12.** Experimental air and water permeation curves for all membranes of different pore sizes.

Source: Author, 2022.

**Table 5.** Average values of air and water permeance for membrane tested.

Sample	Fluid	P (L·h <sup>-1</sup> ·m <sup>-2</sup> ·bar <sup>-1</sup> )
PTFE	air	1954738
PVDF	air	2634755
NF-90	air	428
NF-245	air	43
NF-8038	air	11
PVDF	water	1127
NF-90	water	2
NF-245	water	12
NF-8038	water	7

Pore size/MWCO: PTFE (0.05 μm); PVDF (0.2 μm); NF90 (90 Da); NF245 (245 Da); NF8038 (200 Da).

Source: Author, 2022.

Water flux behavior by transmembrane pressure (range from 0 to 3 bar) in a crossflow system of the membrane samples tested is presented in Figure 13.

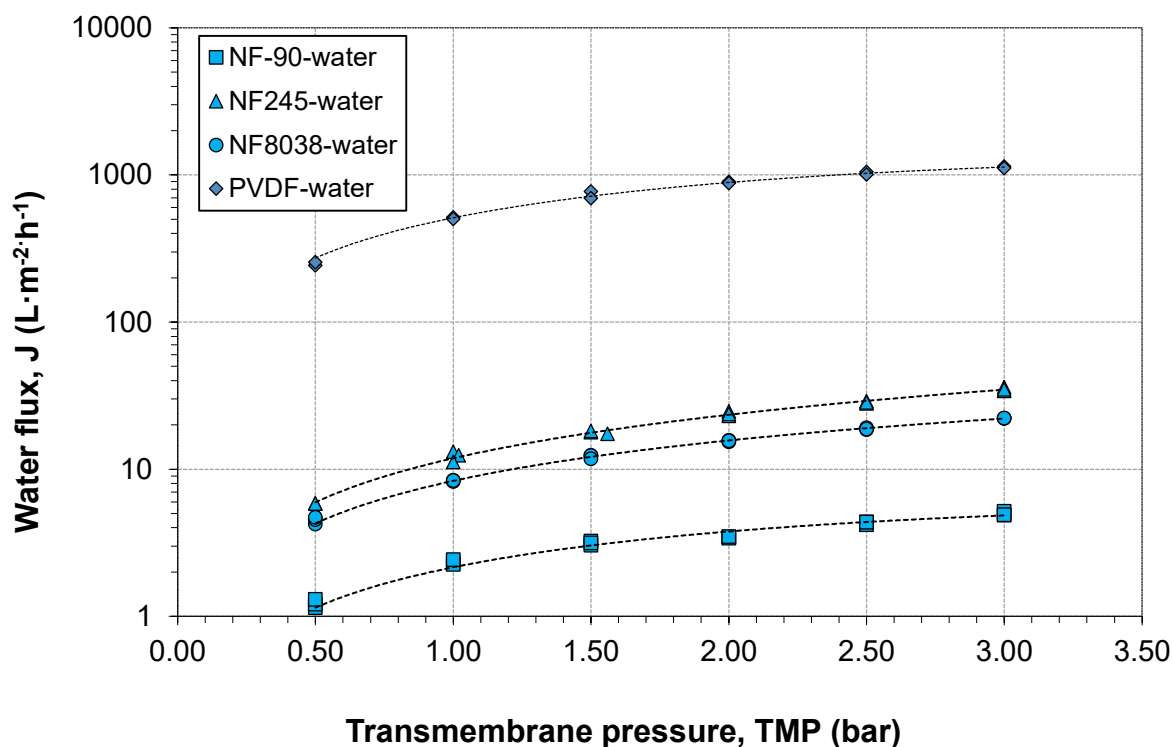


**Figure 13.** Water flux experimental for micro-and nanofiltration membranes.

Note that distilled water flux increases with higher porosity and transmembrane pressure. Das *et al.* (2020) reported the same behavior when studying the fabrication of porous SiC ceramic membrane with different porosity levels from the recycling of coal fly ash. NF-90 exhibited the lowest water flux among all nanofiltration membranes due to its smaller pore size. Nevertheless, NF-90 showed relatively high air permeance compared to the other nanofiltration membranes whose pore size is larger. The dissimilarity may be due to the polarity of the NF-90 membrane. According to Leo *et al.* (2013), the NF-90 membrane presents a water contact angle of 83.4° on a hydrophobic surface. The hydrophobicity and hydrophilicity of the nanofiltration membranes were confirmed with a simple test involving the application of water drop and “on spec” biodiesel drop on the membrane surface. Figure 14 shows the simplified representation of the drop test. The drop of biodiesel and water is represented on the left and right, respectively.

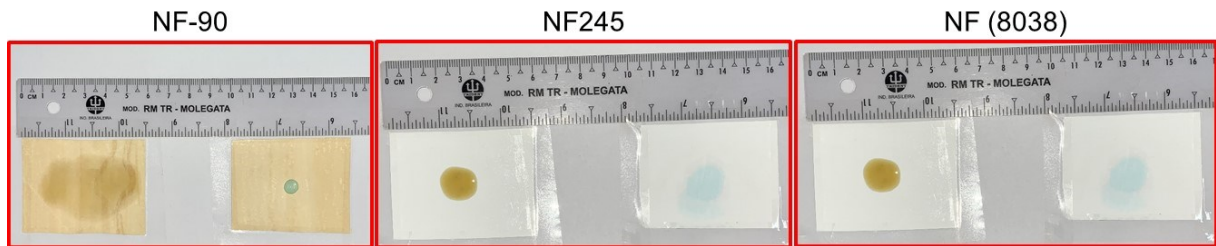


**Figure 14.** Drop test to determine hydrophobic or hydrophilic membrane character.

Source: Author, 2022.

After 1 h, it can be observed that the NF-90 membrane did not soak up the water drop, only the “on spec” biodiesel drop. On the other hand, NF245 and NF8038 completely absorbed the drop of water rejecting biodiesel drop. These results are in agreement with Leo *et al.* (2013) when reporting water contact angles of NF245 and NF8038 of  $11^\circ$  and  $17.2^\circ$ , respectively. Therefore, our results confirm the hydrophilic character of NF245 and NF8038 membranes and the hydrophobic character of NF-90 membrane. Possibly, the NF-90 membrane's hydrophobic character provides a hindrance to water permeation through the pores causing high surface tension showing lowest the water permeance. Air is a fluid without surface tension percolating easily across membrane porous. Indeed, NF245 and NF8038 demonstrate higher water permeance since they are hydrophilic membranes.

In the case of the PTFE membrane, the water permeance test could not be performed as the membrane sample ruptured due to a cutting error and no other samples were available in the laboratory. Similarly, air and water permeance tests were not performed for polyethersulfone membrane (PES with 10 kDa MWCO) because the membrane was stored in a 70% glycerol solution and there was little sample available in the laboratory. Therefore, priority was given to biodiesel testing, which will be discussed in the next section.

### 5.3 “ON SPEC” BIODIESEL PERMEANCE ASSAYS

The biodiesel flux behavior was evaluated regarding the permeance and permeate flux, in a crossflow filtration system, using “on spec” biodiesel.

Membranes with a high water contact angle are recommended in oil filtration since they show higher oil permeance than hydrophilic membranes. Based on this, the NF-90 membrane was the first membrane tested. For the permeation tests, biodiesel within standard specifications was used. Figure 15 shows the visual quality of this biodiesel. The “on spec” biodiesel for permeation tests had the density measured by a pycnometer, presenting a value of  $881.5 \text{ kg/m}^3$  ( $0.881 \text{ g/cm}^3$ ).

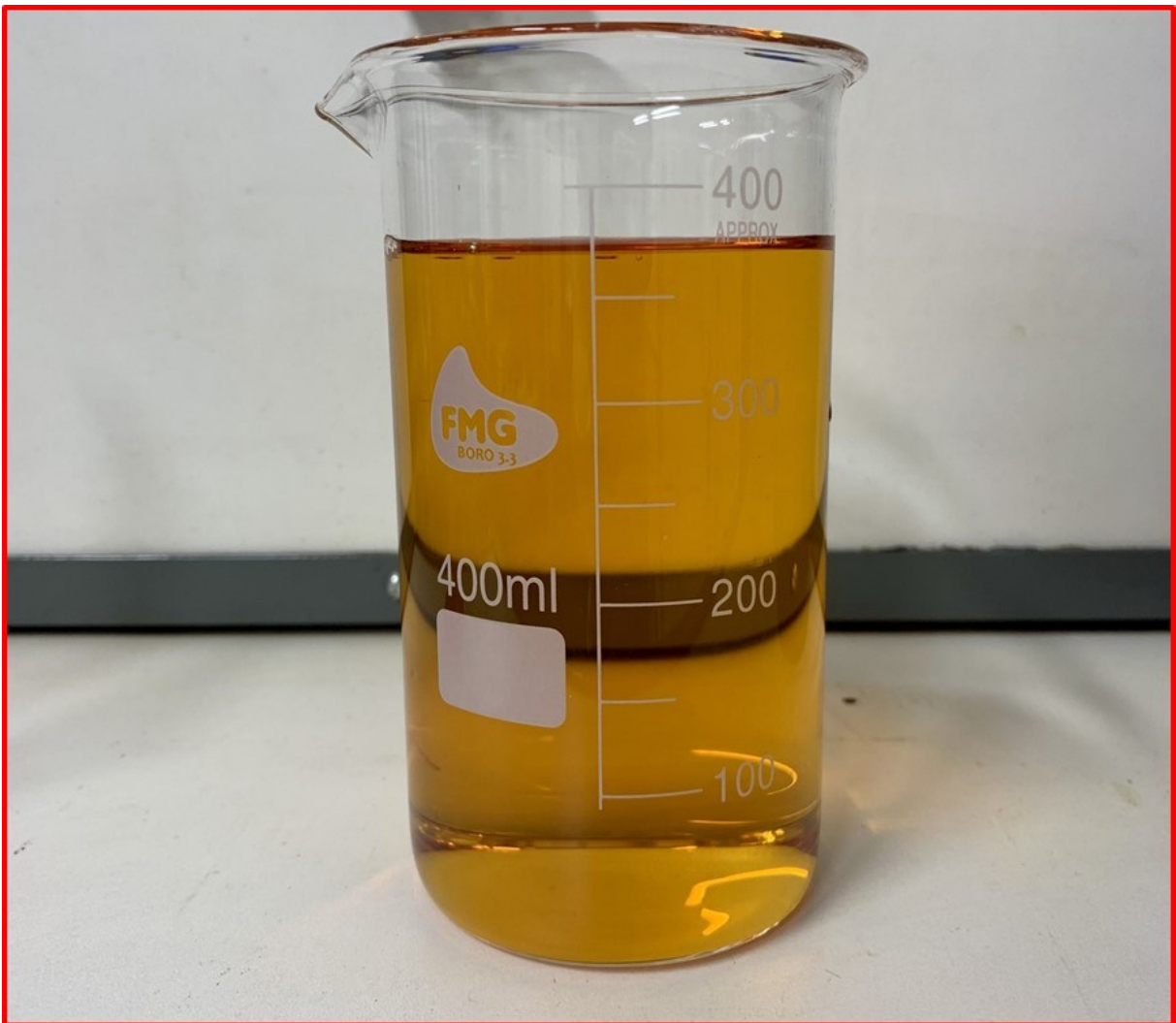


**Figure 15.** “On spec” biodiesel used in permeation assays.

Source: Author, 2022.

Permeate flux (J) and permeance (P) behaviors as a function of the filtering time for the NF-90 membrane are shown in Figure 16. To determine an adequate



experimental time to contact the membrane surface flat with “on spec” biodiesel solution, permeate flux was monitored over time.

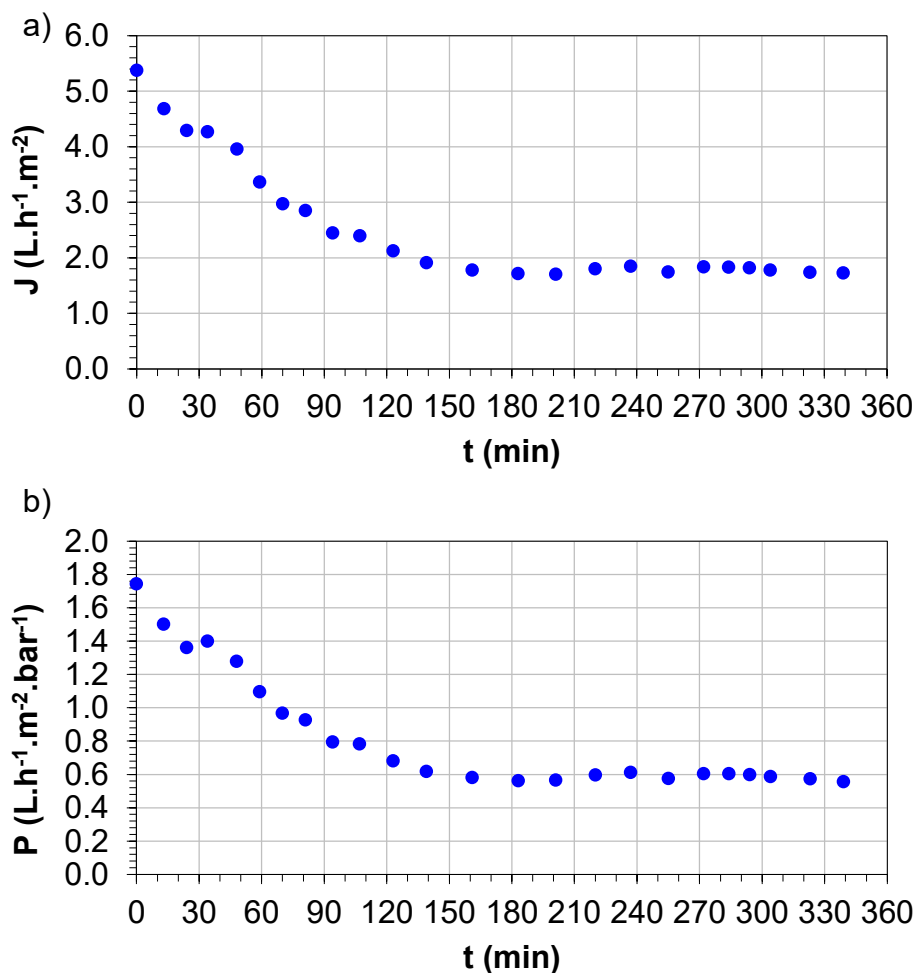


**Figure 16.** Permeate flux (a) and permeance (b) NF90 membrane (90 Da) with “on spec” biodiesel after 360 min of permeation under TMP = 3 bar. The permeate points were collected after 34 min of operation.

Source: Author, 2022.

According to these results, we can observe a typical behavior of the permeate flux over time with an initial decrease within 150 min likely due to fouling and concentration polarization. “On spec” biodiesel may still cause fouling as well within marketing standards its composition includes elements such as mono-, di-, triglycerides, free glycerol, and metals, among others. Subsequently, the permeate flux stabilized after 180 min. According to Choi *et al.* (2005), a possible explanation is due

to the equilibrium of foulant attachment with its detachment between membrane surface and ‘on spec’ biodiesel solution. For polymeric nanofiltration membranes, especially in the tight-NF range, another reason for flux decline is that compaction (due to higher pressure at 3 bar) may alter or decrease the pore size. Permeate collection started after 34 min of contact time between the surface membrane and feed solution. From this time (34 min), 360 min of permeation time was accordingly selected for all experiments for investigating the membrane fouling behavior. In addition, despite the membrane's hydrophobic character, the NF-90 membrane has a relatively low pore size (MWCO 90 Da) which contributes to low permeance.

Figures 17 and 18 represent the permeation flux and permeance behavior of the NF245 and NF8038 membranes, respectively.

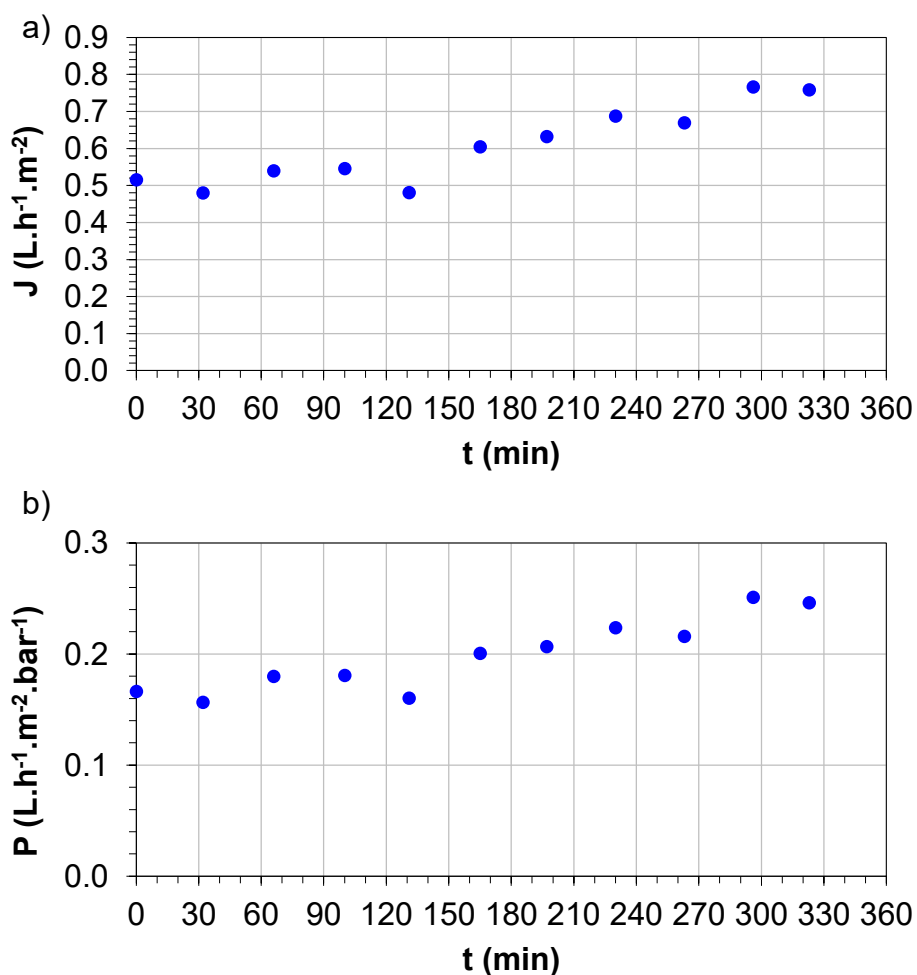


**Figure 17.** Permeate flux (a) and permeance (b) NF245 membrane (245 Da) with “on spec” biodiesel after 360 min of permeation under TMP = 3 bar. The permeate points were collected after 120 min of operation.

Source: Author, 2022.

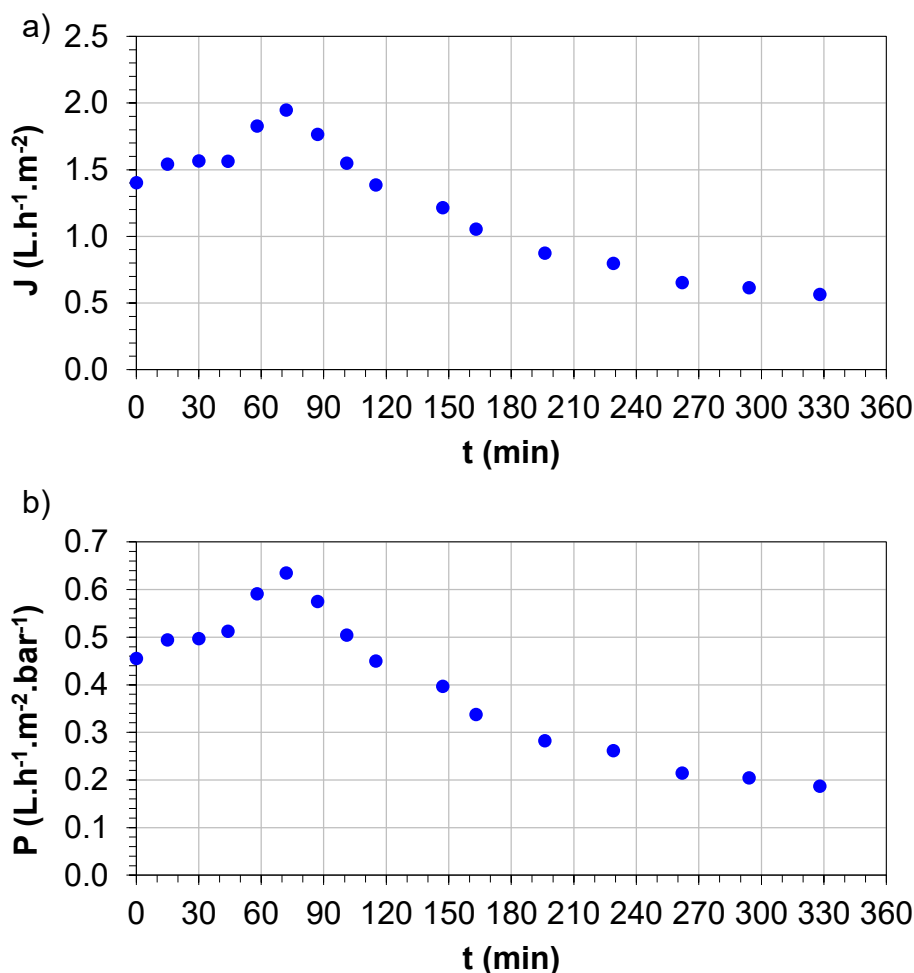


**Figure 18.** Permeate flux (a) and permeance (b) NF8038 membrane (200 Da) with “on spec” biodiesel after 360 min of permeation under TMP = 3 bar. The permeate points were collected after 120 min of operation.

Source: Author, 2022.

Based on the drop test performed earlier, both membranes indicate high hydrophilicity which allows interaction with water instead of “on spec” biodiesel. Among the nanofiltration membranes, the highest water permeance was achieved using the hydrophilic NF245 membrane as shown in Table 4. On the other hand, it showed the lowest permeance for biodiesel and, consequently, the lower permeate flux. Permeance values for NF245 and NF8038 membranes were 0.17 L·h<sup>-1</sup>·m<sup>-2</sup>·bar<sup>-1</sup> and 0.46 L·h<sup>-1</sup>·m<sup>-2</sup>·bar<sup>-1</sup>, respectively. Although NF245 presents a higher pore size (or

MWCO) when compared with NF8038, it exhibited lower “on spec” biodiesel permeance. This may be due to two factors. First, the higher hydrophilicity of the NF245 membrane provides a hindrance to “on spec” biodiesel percolation through the pores due to the low water contact angle ( $\sim 11.0^\circ$ ). Second, based on the report of Dolar *et al.* (2012), NF8038 presents bimodal pore-size distribution with small pores size of 1.04 nm and large pores size ranging from 1.3 to 2.1 nm. Therefore, the higher permeance of the NF8038 membrane compared with NF245 may be due to large pores. Due to its hydrophobic character, the NF-90 membrane showed the highest permeation to biodiesel among the nanofiltration membranes.

Generally, membranes with hydrophilic and smooth surfaces are more appropriate for oil filtration because they are less vulnerable to fouling (LEO *et al.*, 2013). From the permeation graph (Figure 17) of the NF245 membrane, a constant flux is observed at the beginning and subsequent increase throughout the permeation period (360 min). Nevertheless, a different behavior occurred with the NF8038 membrane. There is an increase in the permeation flux between 60 to 90 min. Most likely, this represents the time for membrane conditioning and membrane swelling occurred. After membrane swelling, a decrease in permeation flux occurred, showing the fouling tendency of the membrane. There was no apparent chemical damage between membrane material and biodiesel. Figure 20 shows the integrity of the membrane surface after “on spec” biodiesel tests.

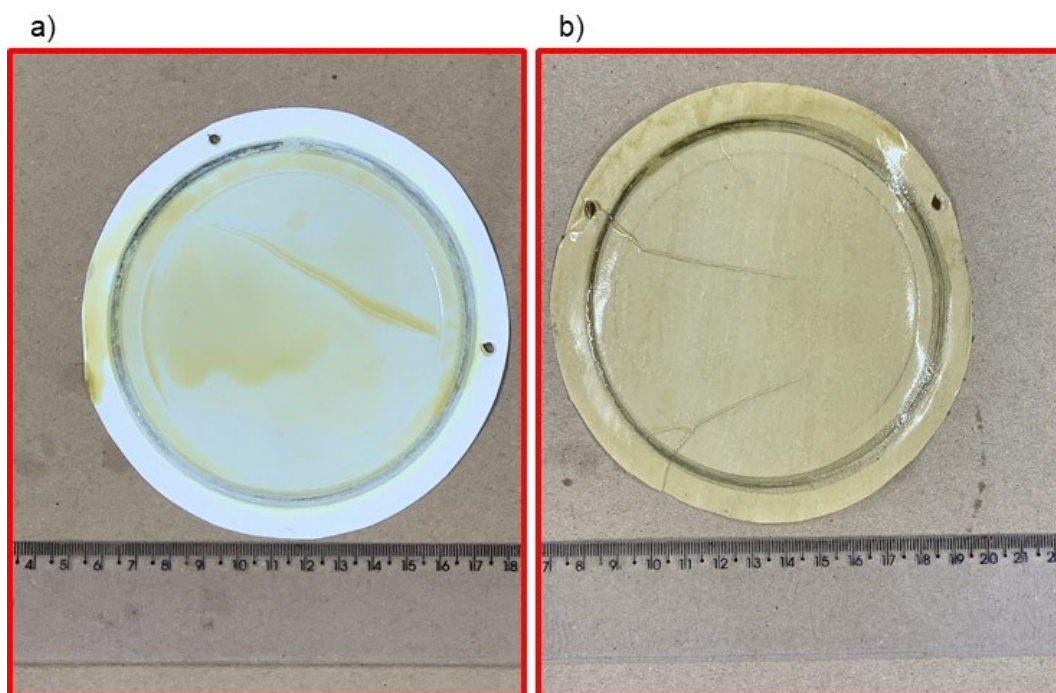


**Figure 19.** Membrane surface after permeation tests with “on spec” biodiesel: (a) NF245 and (b) NF-90.

Source: Author, 2022.

Figures 20 (a) and (b) represent the permeation flux and permeance behavior of the microfiltration PVDF membrane.

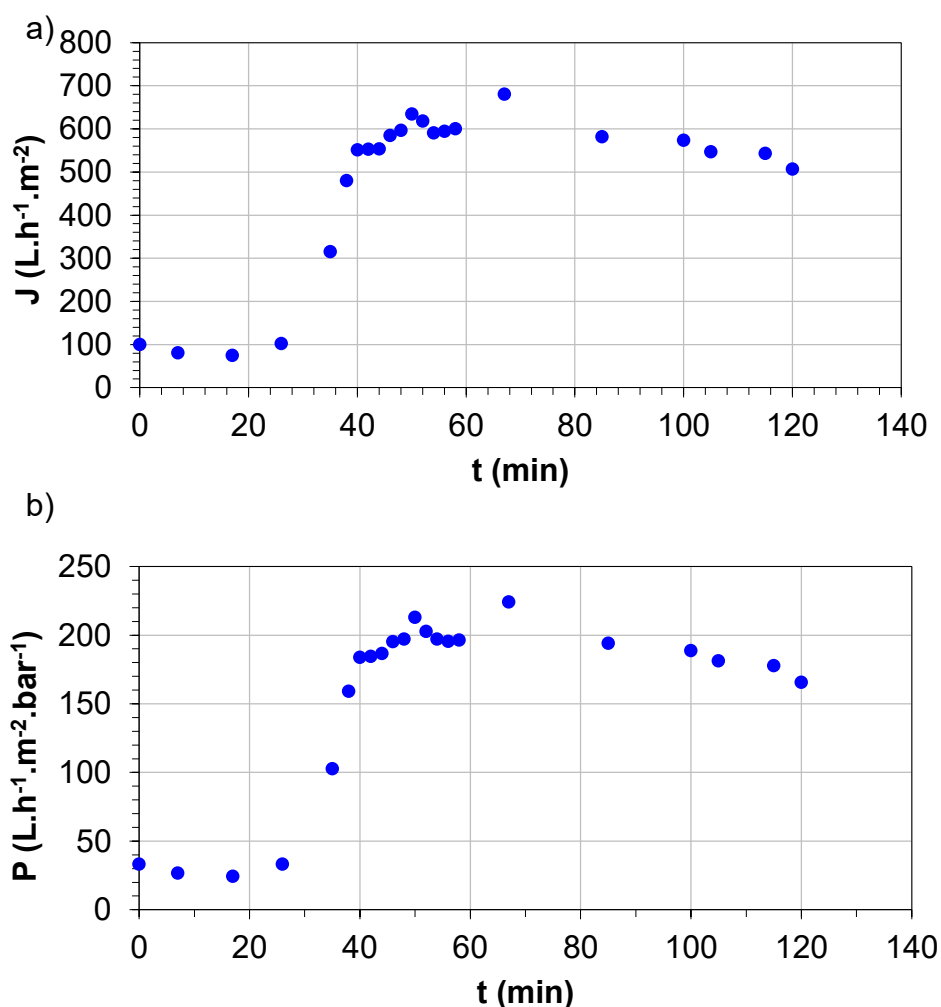


**Figure 20.** Permeate flux (a) and permeance (b) PVDF membrane (0.2  $\mu\text{m}$ ) with “on spec” biodiesel after 120 min of permeation under TMP = 3 bar. The permeate points were collected immediately after the start of the operation.

Source: Author, 2022.

The experimental permeation curve as a function of time shows an increase in the initial flux in the first 40 min of operation for the membrane of 0.2  $\mu\text{m}$ . This behavior can be explained as the time required for membrane conditioning and swelling. After this time, the flux tends to stabilize until reaching low variations. The flux obtained is greater with the more open membrane with high permeances from 550 to 680  $\text{L}\cdot\text{h}^{-1}\cdot\text{m}^{-2}$ . Figure 21 shows the surface of the PVDF membrane after permeation in “on spec” biodiesel.



**Figure 21.** PVDF Membrane surface after permeation tests with “on spec” biodiesel.

Source: Author, 2022.

In the “on spec” biodiesel permeation using the polyethersulfone (PES) membrane, different permeate fluxes were obtained. The results are presented in Figures 22, 23, and 24. The reason for the three tests will be discussed in the next section.

The initial fluxes were slightly the same, confirming the reproducibility of laboratory tests. As already mentioned, the “on spec” biodiesel was used to promote conditioning on the membrane for improving pore wetting with the FAME in the filtration process. In all permeations using the ultrafiltration polyethersulfone (PES) membrane, the flux increased regularly in time. This result can be explained by pore dilatation caused by membrane swelling with the biodiesel, i.e., the first 2 hours represent the time required for membrane pores conditioning. Low flux variation is observed after the conditioning time.

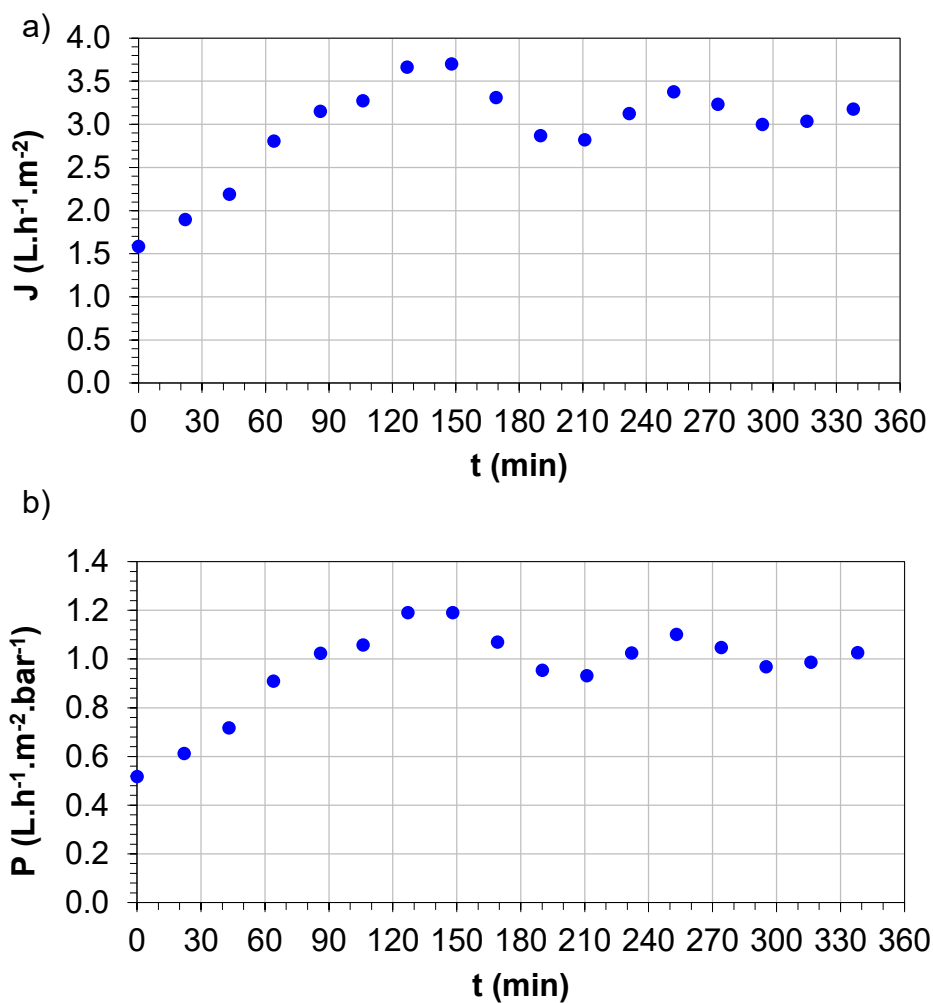


**Figure 22.** Permeate flux (a) and permeance (b) PES membrane (10 kDa) with “on spec” biodiesel during 360 min permeation under TMP = 3 bar (conditioning for the first filtration test with industrial FAME). The permeate points were collected after 120 min of operation.

Source: Author, 2022.



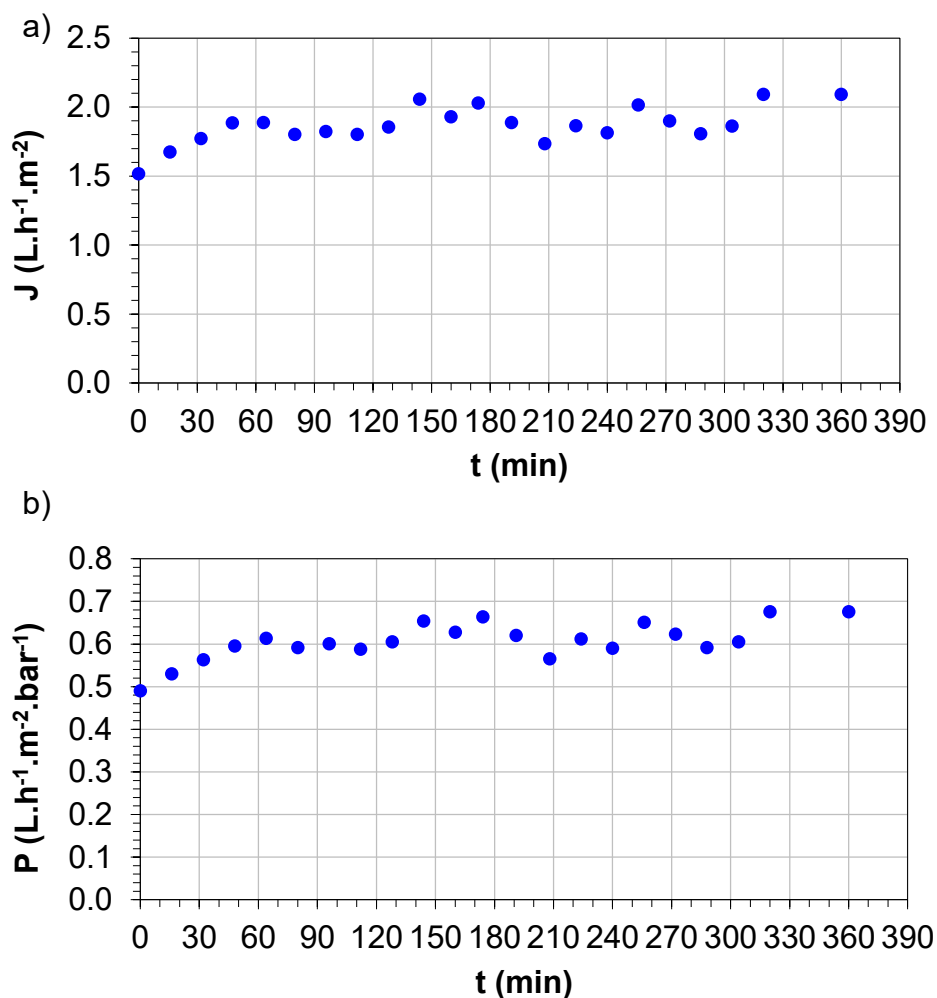


**Figure 23.** Permeate flux (a) and permeance (b) PES membrane (10 kDa) with “on spec” biodiesel during 360 min permeation under TMP = 3 bar (conditioning for the second filtration test with industrial FAME). The permeate points were collected after 120 min of operation.

Source: Author, 2022.

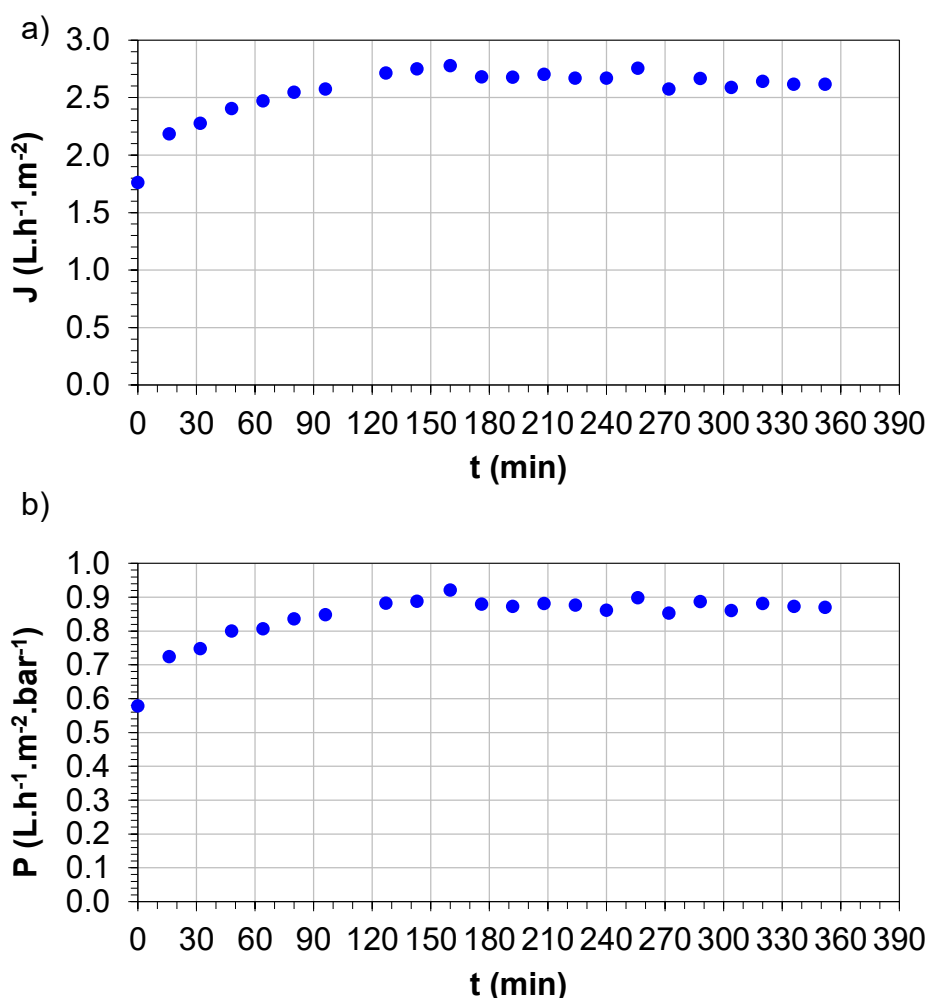


**Figure 24.** Permeate flux (a) and permeance (b) PES membrane (10 kDa) with “on spec” biodiesel during 360 min permeation under TMP = 3 bar (conditioning for the third filtration test with industrial FAME). The permeate points were collected after 120 min of operation.

Source: Author, 2022.

The ultrafiltration polyethersulfone membrane with MWCO of 10 kDa presented an average permeate flux of  $1.62 \text{ L}\cdot\text{h}^{-1}\cdot\text{m}^{-2}$  and permeance of  $0.53 \text{ L}\cdot\text{h}^{-1}\cdot\text{m}^{-2}\cdot\text{bar}^{-1}$ . Possibly, the low permeation rate is due to the hydrophilic membrane feature. On the other hand, the results obtained in the first permeation test (Figure 20) were shown slightly different behavior when compared to the two subsequent tests (Figures 23 and 24). Permeation tests were made with different pieces of the same membrane. Note that both permeate flux and permeance presented higher values. This fact may be due

to small pressure and temperature variations in the device. During the experiment, it was found that a long time was taken for collecting the first permeate drop, an average time of 2 h. The results related to the filtration tests with industrial biodiesel will be presented in the next section.

#### *5.4 FILTRATION PERFORMANCE FOR FAME POLISHING USING POLYMERIC MEMBRANE*

The real industrial enzymatic FAME samples used in the polishing with membranes mentioned previously had high contents of soaps, acidity, and moisture, among other contaminants, and represent a new and interesting challenge. The permeance study gives us the prior information about the flow behavior of each of the membranes. Based on this, similar behavior is expected for the real industrial FAME samples.

The first membrane tested was NF-90. This membrane was chosen according to hydrophobicity, i.e., its capacity to absorb FAME and repel water. Moreover, NF-90 showed the shortest time to permeate the first drop. Besides membrane characteristics, some factors such as temperature, transmembrane pressure, and acidified water content can have a significant impact on the filtration process. Many data in the literature claim that the addition of acidified water improves the biodiesel separation process. It is worth mentioning in this work no acidified water was added because our real industrial enzymatic FAME samples already present water as a consequence of the transesterification process itself.

Despite the good permeance shown in the previous “on spec” biodiesel tests, NF-90 membrane results were unsatisfactory because it did not permeate with industrial FAME for up to 6 hours. As mentioned earlier, this result occurred due to the NF-90 membrane's low pore size. In addition, there was no permeation with any nanofiltration membrane due to the low-pressure gradient used. In Figure 25, it can be observed that the dry membrane module, as well as the underside of the membrane, is dry (non-bright surface) proving the non-permeation of industrial FAME. In the sequence, Figure 26 shows the surface of the NF-90 membrane after attempted separation.



**Figure 25.** Dry membrane module after filtration test.

Source: Author, 2022.



**Figure 26.** Surface NF-90 membrane after contact with industrial FAME in separation attempt.

Source: Author, 2022.

Subsequently, the membrane that was tested was a polyvinylidene fluoride membrane. While operating the equipment it was noted that the polyvinylidene fluoride membrane was completely permeable for the industrial FAME even without a pressure transmembrane. Permeates remained with the same dark coloration as the feed samples. Thus, it was concluded that the 0.2- $\mu\text{m}$  PVDF membrane in its natural form, e.g., without modifications, was not suitable for industrial FAME polishing. Figure 27 shows the integrity of the PVDF membrane surface after filtration tests with industrial FAME.

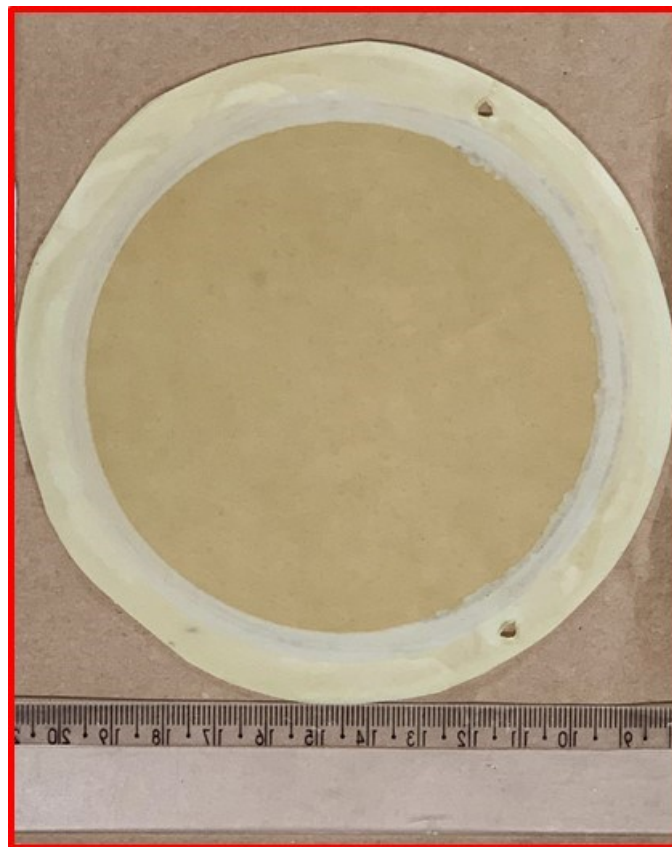


**Figure 27.** PVDF Membrane surface after permeation tests with industrial FAME.

Source: Author, 2022.

The 10-kDa UF PES membrane was successfully used for industrial FAME polishing. Alves *et al.* (2013), demonstrated that the 10 kDa PES membrane (GE Osmonics, USA) was able to reduce the glycerol content in biodiesel obtained from refined soybean oil. According to Sokac *et al.* (2020), glycerol was successfully

separated by UF 10 kDa PES membrane (Millipore, Germany) from biodiesel produced by lipase-catalyzed transesterification with an efficiency of 83.83%.

In the experiments performed in this work, the UF PES membrane was tested in three processes. First, the PES membrane was preconditioned by 6 h in “on spec” biodiesel with permeation curve (achieved during conditioning) shown in Figure 22 (Section 5.3). Then, the membrane was submitted to the filtration process with industrial FAME. As mentioned before, the operating conditions were a pressure gradient of 3 bar, and room temperature around 25 °C in a crossflow system. Figure 29 presents the flux of industrial FAME through the UF membrane. Although the process is pressure-driven, the ultrafiltration membrane flux was low and a flux constancy was observed in this case. The flux stabilizes after 60 min. No decline in flux due to fouling was observed over 280 min of filtration.

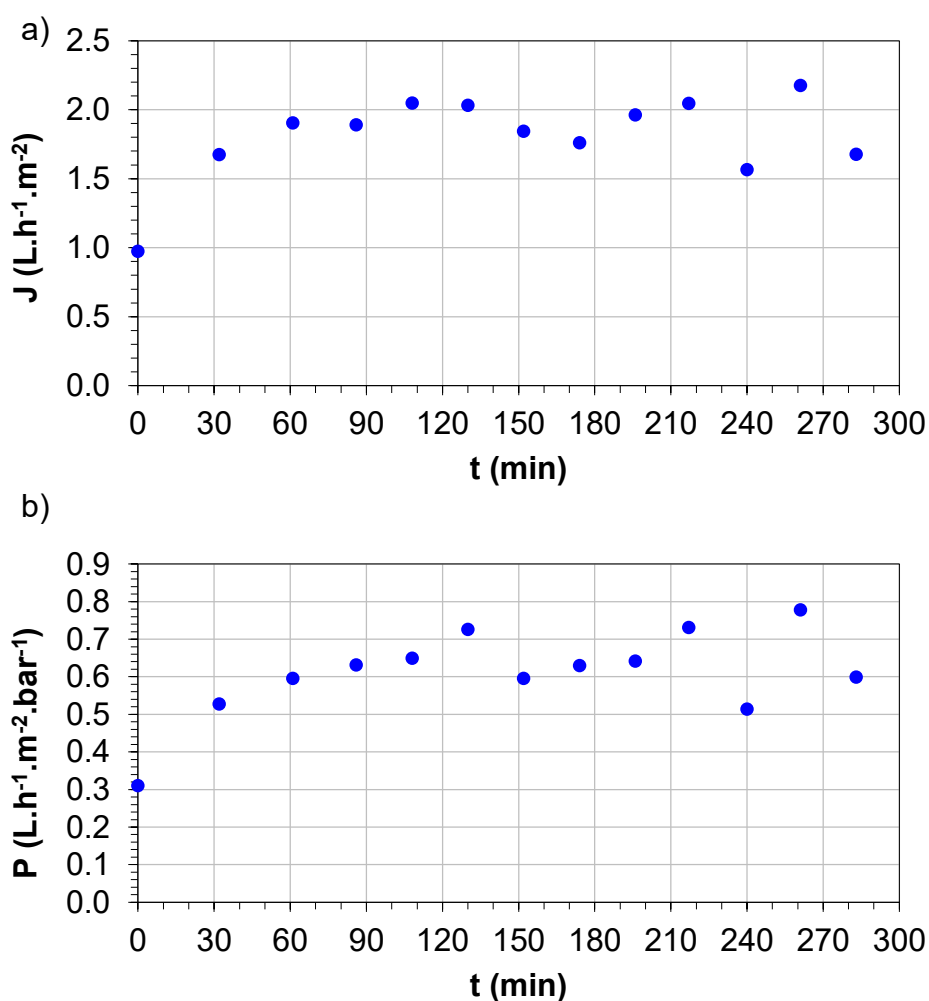


**Figure 28.** Permeate flux (a) and permeance (b) PES membrane with industrial FAME (sample 467) after 280 min of permeation under TMP = 3 bar.

Source: Author, 2022.

Figure 29 depicts the results FAME sample 467 permeation. Firstly, using a graduated pipette, the crude FAME sample was removed and stored in a 1000 mL Erlenmeyer. Then, the system was put into operation under the above-mentioned process conditions and the permeate was collected.

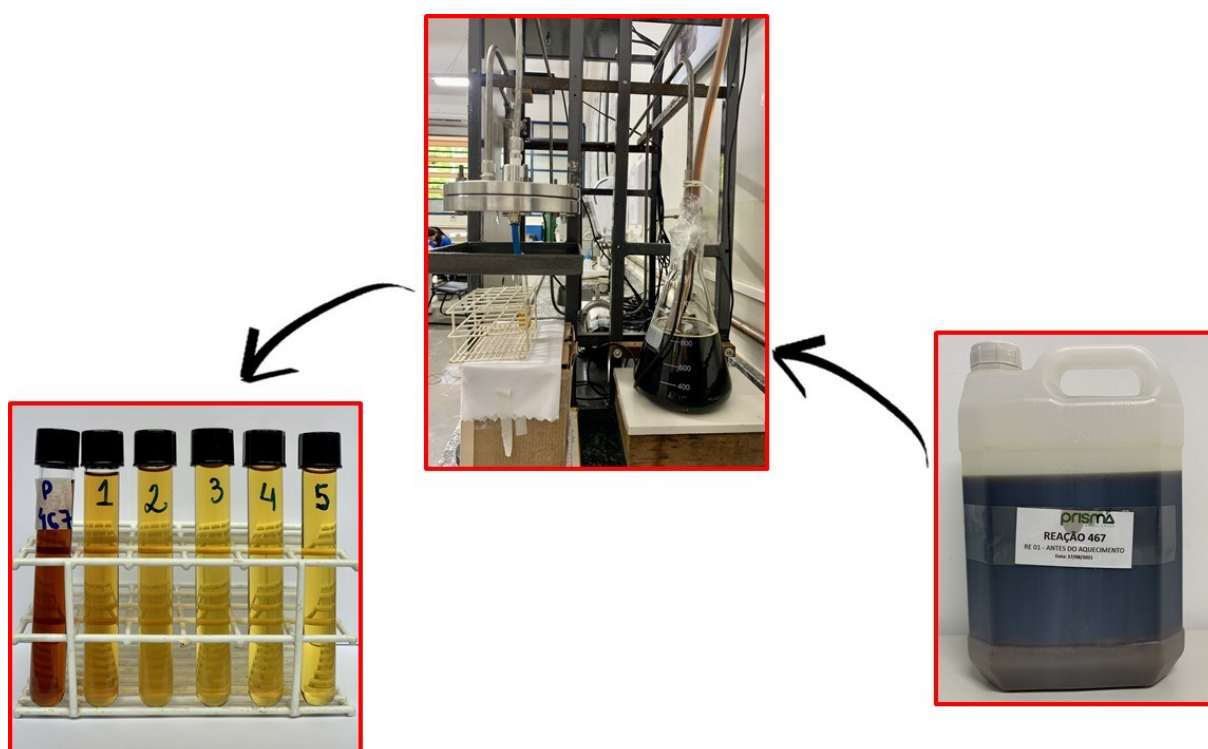


**Figure 29.** Schematic representation of the steps for obtaining permeates.

Source: Author, 2022.

The clarified permeates obtained indicate the efficiency of the membrane in separating the contaminants present in industrial FAME. The permeate samples were quantitatively evaluated, as shown in Table 6. The collected permeates were labeled with a number ranging from 1 to 19, indicating that each number in the table corresponds to a volume of 13 ml collected and stored in test tubes with a cap.

**Table 6.** Soap, acidity, and moisture content after ultrafiltration with polyethersulfone membrane.

<b>Sample</b>	<b>Soap (ppm)</b>	<b>Acidity (%)</b>	<b>Moisture (ppm)</b>
1	n.d.	3.39	2793
2	n.d.	2.13	1380
3	n.d.	2.76	1652
4	n.d.	2.94	1677
5	n.d.	2.95	1734
6	n.d.	3.01	2799
7	n.d.	3.45	1959
8	n.d.	2.99	1828
9	n.d.	3.18	1724
10	n.d.	2.91	1767
11	n.d.	3.67	1649
12	n.d.	3.30	4406
13	n.d.	3.54	5401
14	n.d.	3.50	5412
15	n.d.	3.68	5463
16	n.d.	3.74	2374
17	n.d.	3.42	6379
18	n.d.	3.60	6251
19	n.d.	3.57	6694

n.d.: Not detected

<sup>a</sup> Composition of industrial FAME: Soap (558 ppm); Acidity (4.54%), and Moisture (7000 ppm).

As it can be seen, UF 10 kDa PES membrane was efficient in soap removal, since all samples were free from soaps. The membrane permeation also decreased acidity content, although at a lower level. The moisture content was reduced in all samples, but in the last permeates the reduction ratio decreased. This fact may be related to possible fouling on the membrane surface, thus decreasing the membrane efficiency. In addition, over time, the membrane gets wet with water, and the water flux increases. Figure 30 shows the integrity of the flat sheet membrane after 280 min of filtration at a transmembrane pressure of 3 bar. Note that, although we used a real FAME sample, there was no qualitatively apparent chemical damage with the membrane material.



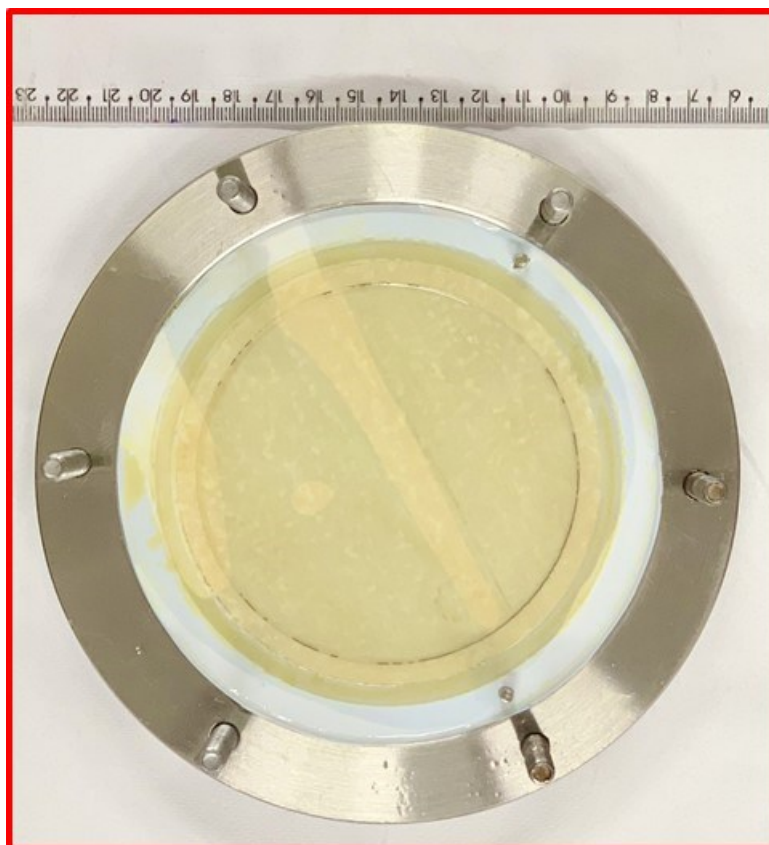


**Figure 30.** Membrane surface after direct contact with real industrial FAME for 280 min in a crossflow filtration system at 3 bar.

Source: Author, 2022.

To validate the experimental results obtained in Table 5, another test was performed with the same sample of industrial FAME (sample 467). It is worth mentioning that each membrane was used only once and then discarded, i.e., a new membrane sample was used for each filtration test. Following our standard method, a new flat membrane disk was subjected to preconditioning with “on spec” biodiesel, and the permeation curves were shown in Figure 23 (Section 5.2). Then, the membrane was submitted to the filtration process with industrial FAME.

To determine a proper experimental time to contact the membrane with feed industrial FAME and at the same time simulate a continuous industrial process, a new filtration experiment was conducted for 12 h and the flux was monitored over time. The flux results obtained for the 10 kDa PES membrane are presented in Figure 31.

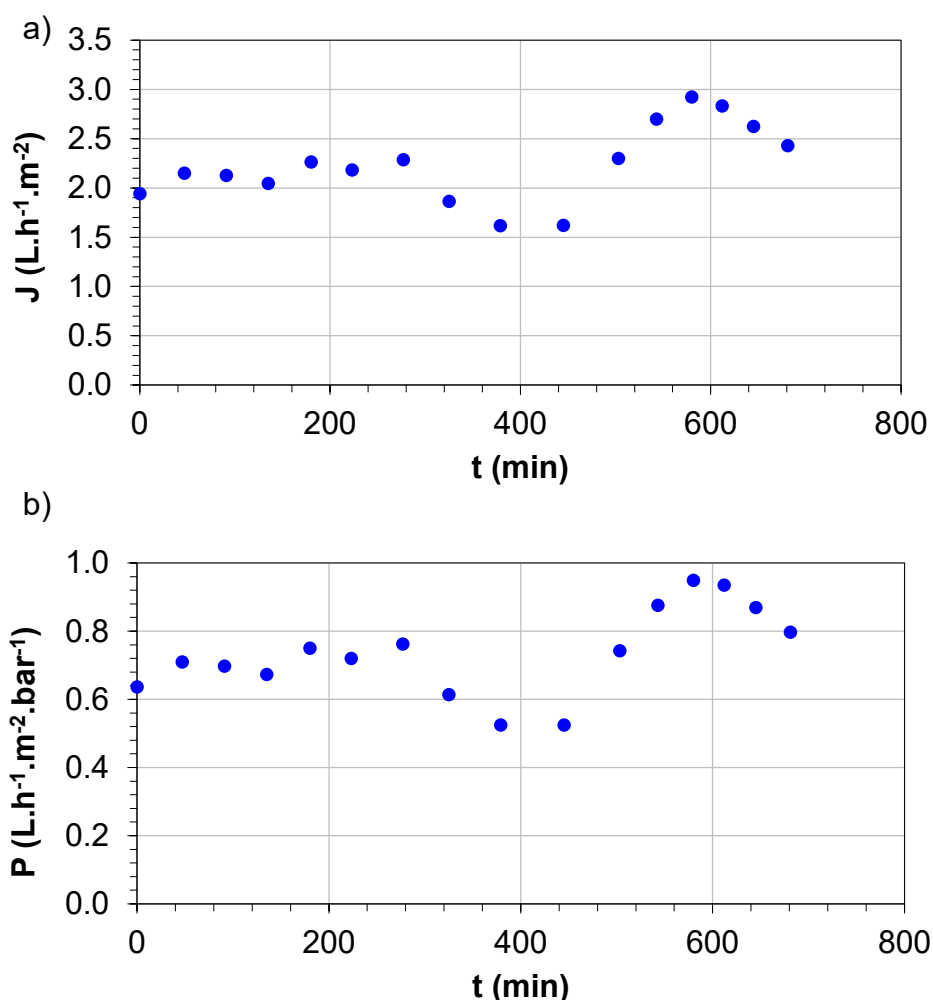


**Figure 31.** Permeate flux (a) and permeance (b) 10 kDa PES membrane with industrial FAME (sample 467) after 12 h of permeation under TMP = 3 bar.

Source: Author, 2022.

There is a slight increase in flux around 540 min of filtration. This behavior can be explained by a pressure drop in the retentate outlet pipe. At one point during the filtration operation, the suction hose from the FAME feed stuck to the glass part of the Erlenmeyer causing a sudden pressure drop, and consequently rupture in the membrane surface. The pressure stabilized, the membrane was not removed from the module, and the filtration process was not stopped. Despite this issue, the permeate samples continued to be collected. Figure 32 shows the membrane surface after 12 h of filtration.

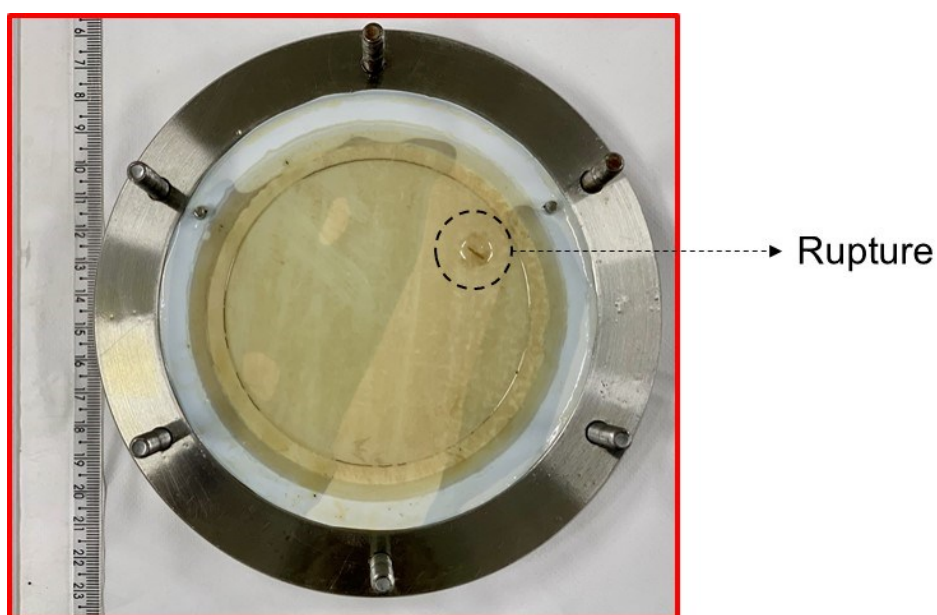


**Figure 32.** Membrane surface after direct contact with real industrial FAME for 12 h in a crossflow permeation system at 3 bar.

Source: Author, 2022.

The permeates obtained in the second filtration process with FAME sample 467 are presented in Figure 33. Flask 1 and 2 correspond to feeding and retained, respectively. The samples were quantitatively analyzed in terms of soap, acidity, moisture, and color, as shown in Table 7.



**Figure 33.** Permeates obtained during 12 h of filtration.

Source: Author, 2022.

**Table 7.** Soap, acidity, moisture content, and color after ultrafiltration with the 10 kDa PES membrane.

<b>Sample</b>	<b>Soap (ppm)</b>	<b>Acidity (%)</b>	<b>Moisture (ppm)</b>	<b>Color (gardner)</b>
1	n.d.	3.36	6000	10.9
2	n.d.	4.36	1030	10.9
3	n.d.	4.17	1730	10.9
4	n.d.	4.76	4300	10.9
5	n.d.	4.31	6000	10.9
6	n.d.	4.31	4500	10.9
7	n.d.	4.62	7300	10.9
8	n.d.	3.68	3900	10.9
9	n.d.	3.76	4300	10.9
10	n.d.	3.99	3800	10.9
11	n.d.	4.15	4000	10.9
12	n.d.	4.45	4000	10.9
13	n.d.	3.95	3100	10.9
14	n.d.	3.69	4300	10.9
15	n.d.	4.81	5200	10.9
16	n.d.	4.50	3100	10.9

n.d.: Not detected

<sup>a</sup> Composition of industrial FAME: Soap (558 ppm); Acidity (4.54%); Moisture (7000 ppm), and Color: 16.

This process was also efficient, mainly, for soap and color removal since in all permeate samples, no soap was detected, and color was reduced. This result contributes to improving the appearance of biodiesel. A decrease in water and acidity contents was detected, but it was not significant.

The final sample that was tested was sent by a partner industry in Erechim, RS, Brazil. This sample took place analysis of total contamination and phosphorus content, besides soap, acidity, moisture, and color levels. The permeation results of the FAME industrial sample are presented in Figure 34.



**Figure 34.** Schematic representation of the steps for obtaining permeates from the industrial sample.

Source: Author, 2022.

The membrane permeation was highly efficient in polishing the FAME industrial sample. The permeates presented a good visual aspect, bright and clear. The objective proposed for the sample in question was to analyze the levels of total contamination. Thus, a large volume of collected permeate was required. In this way, the filtration system operated for ~70 h. It was not a continuous operation, i.e., at the end of the day, the equipment was turned off and restarted the next day in the morning. Hence, the initial procedure was to precondition the membrane in “on spec” biodiesel, providing the permeation and permeance curves of Figure 24. In the sequence, crude FAME was filtered through the UF PES membrane. Figure 35 presents the flux of FAME across the UF 10 kDa membrane at 3 bar.

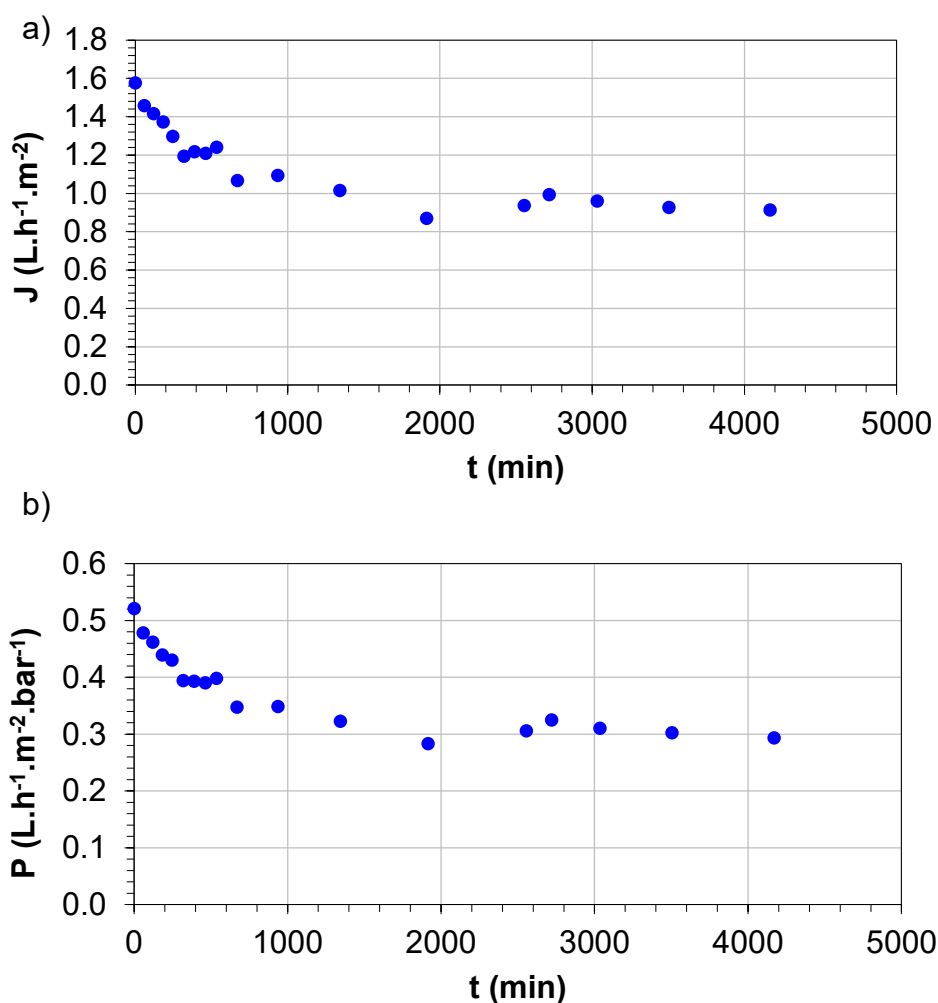


**Figure 35.** Permeate flux (a) and permeance (b) PES membrane with industrial FAME (sample Erechim) after 70 h of permeation under TMP = 3 bar.

Source: Author, 2022.

As shown in Figure 35, an initial decrease in permeate flux of UF 10 kDa PES membrane was observed. Then, the permeate flux started to stabilize, probably due to fouling and concentration polarization blocking membrane pores, which increased the membrane resistance. During crossflow filtration, a layer may be formed by the accumulation of hydrophilic compounds on the membrane surface forming large droplets (ATADASHI et al., 2015). Figure 36 shows the membrane surface after 70 h of filtration.



**Figure 36.** Membrane surface after direct contact with real industrial FAME for 70 h in a crossflow filtration system at 3 bar.

Source: Author, 2022.

Soap, acidity, moisture, color, and total contamination levels in all permeate sample during the UF with 10 kDa PES membrane is presented in Table 8.

**Table 8.** Soap, phosphorus, acidity, moisture content, color, and total contamination after UF with 10 kDa PES membrane.

Sample	Soap (ppm)	Phosphorus (mg/kg)	Acidity (%)	Moisture (ppm)	Color (gardner)
1	n.d.	0.51	1.99	1148	10
2	n.d.	0.51	2.03	1250	10
3	n.d.	0.51	1.90	1225	10
4	n.d.	0.51	1.88	1201	10
5	n.d.	0.51	1.69	910	10
6	n.d.	0.51	1.63	904	10
7	n.d.	0.51	1.60	902	10
8	n.d.	0.51	1.62	905	10
9	n.d.	0.51	1.56	893	10
————— Total Contamination <sup>b</sup>				0.58	mg/kg

n.d.: Not detected

<sup>a</sup> Composition of industrial FAME: Soap (449.5 ppm); Acidity (2.14%); Moisture (1018 ppm), Phosphorus (16.89 mg/kg); and Color: 12.8

<sup>b</sup> Total Max. Contamination: 24 mg/kg

The same trend was observed for all filtration tests and no soap was detected in all permeate samples. Generally, the mechanism of separation of soap and water from FAME by UF PES membrane is associated with two factors: water immiscibility in biodiesel and soap surface activity. The soap exists in the form of reversed micelle and for this reason, the hydrophilic side of the soap is bound to the droplets of water. On the other hand, the hydrophobic side is submerged in the biodiesel. As a consequence, the reversed micelle of water and soap is too large to pass through the membrane pores, and therefore easily retained by the biodiesel membrane separation process (ATADASHI et al., 2015; WANG et al., 2009). Another factor that may be associated with the mechanism of mass transfer through the membrane pores is the fact that if the pressure gradient through the membrane increases, biodiesel droplets can change their shape and, consequently, they will cross through the membrane pores (NORIEGA; NARVÁEZ; HABERT, 2018).

The biodiesel color standard is 10 on the Gardner color scale, proving the adequate result obtained. Total contamination was another value presented with excellence since total contamination according to the ASTM standard reaches a maximum value of 24 mg/kg. The membrane was so efficient in this parameter that it exhibited a value of 0.58 mg/kg. The phosphorus content of the permeates showed a considerable reduction, around 97% for all samples meeting the specifications established by ASTM. From Figures 37 and 38, it is possible to observe the high visual quality of the permeates obtained after biodiesel UF.



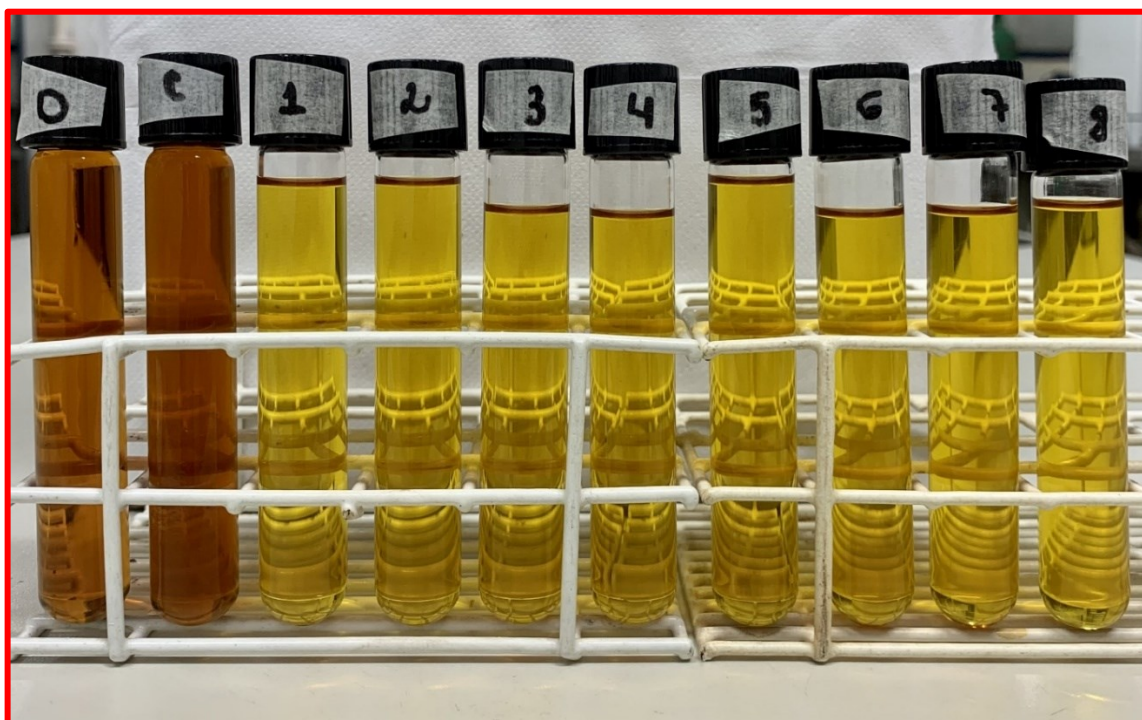


**Figure 37.** Quality permeates obtained by ultrafiltration polyethersulfone. Feed and concentrate (retained) are represented by O and C, respectively.

Source: Author, 2022.



**Figure 38.** Fatty acid methyl ester obtained after polishing through UF with 10 kDa PES membrane.

Source: Author, 2022.

## 6 CONCLUSIONS AND PERSPECTIVES

This work evaluated the application of micro-, ultra-, and nanofiltration membranes for biodiesel polishing. Membranes were evaluated based on permeate flux, permeance behavior (to air, water, and “on spec” biodiesel), soap, acidity, moisture, color, and total contamination contents in the permeate. The permeance tests confirm the trend towards higher air permeance values compared to lower liquid fluid permeance values (water and “on spec” biodiesel) due to the surface tension that hinders the liquid percolation through the pores. Microfiltration polyvinylidene difluoride (PVDF) membrane was completely permeable for the industrial FAME while nanofiltration membranes did not achieve permeation for industrial biodiesel at the 3 bar pressure used. Among the analyzed membranes, the 10 kDa PES membrane was efficient in soap removal, and in all samples, no soap was detected. The membrane permeation made caused excellent color removal and the permeate achieved good levels within the Gardner scale color standard. Furthermore, the permeate reached total contamination and phosphorus levels down to 0.58 and 0.51 mg/kg, respectively, meeting the standard specifications established by ASTM. This membrane (10 kDa PES) presented a mean permeate flux of 1.74 L/h·m<sup>2</sup> for industrial FAME. However, the differences between the permeate flux for each filtration test performed are due to the different feedstocks used in the production of the biodiesel samples. In the present work, we could obtain a decrease in moisture and acidity levels of an industrial FAME. Although the final concentration of water (lowest value obtained was 893 ppm) and acidity (lowest value obtained was 1.56%) still do not meet ASTM standard specifications (less than 200 ppm for water and less than 0.50% for acidity), the use of ultrafiltration with a 10 kDa PES membrane is a suitable alternative for fatty acid methyl ester polishing. The use of a 10 kDa PES membrane could decrease the number of stages required to reach biodiesel specifications, reducing costs and increasing process productivity.

## REFERENCES

- ALVES, M. J. et al. Biodiesel purification using micro and ultrafiltration membranes. **Renewable Energy**, v. 58, p. 15–20, 2013.
- ASTM, D.-00. Standard Test Method for Determination of Water in Petroleum Products, Lubricating Oils, and Additives by Coulometric Karl Fisher Titration. In: **Petroleum Products, Liquid Fuels, And Lubricants (II): D4177 – D6468**. [s:L: s.n.]. p. 5
- ASTM, D.-07. Standard Test Method for Acid Number of Petroleum Products by Potentiometric Titration. In: **Petroleum Products, Liquid Fuels, And Lubricants (II): C1234 – D4176**. 05.01 ed. [s:L: s.n.]. p. 8.
- ASTM, D.-11. Standard Test Method for Water and Sediment in Fuel Oils by the Centrifuge Method (Laboratory Procedure). In: **Petroleum Products, Liquid Fuels, And Lubricants (II): C1234 – D4176**. 05.01 ed. [s:L: s.n.]. p. 7.
- ASTM, D.-20A. Standard Specification for Biodiesel Fuel Blend Stock (B100) for Middle Distillate Fuels. In: **Petroleum Products, Liquid Fuels, And Lubricants (III): D6469 – D7398**. 05.03 ed. [s:L: s.n.]. p. 11.
- ATADASHI, I. M. et al. Refining technologies for the purification of crude biodiesel. **Applied Energy**, v. 88, n. 12, p. 4239–4251, 2011.
- ATADASHI, I. M. et al. High quality biodiesel obtained through membrane technology. **Journal of Membrane Science**, v. 421–422, p. 154–164, 2012.
- ATADASHI, I. M. et al. Removal of residual palm oil-based biodiesel catalyst using membrane ultra-filtration technique: An optimization study. **Alexandria Engineering Journal**, v. 53, n. 3, p. 705–715, 2014.
- ATADASHI, I. M. et al. Crude biodiesel refining using membrane ultra-filtration process: An environmentally benign process. **Egyptian Journal of Petroleum**, v. 24, n. 4, p. 383–396, 2015.
- ATADASHI, I. M.; AROUA, M. K.; AZIZ, A. A. Biodiesel separation and purification: A

review. **Renewable Energy**, v. 36, n. 2, p. 437–443, 2011.

BARNICKI, S. D.; FAIR, J. R. Separation system synthesis: a knowledge-based approach. 1. Liquid mixture separations. **Industrial & Engineering Chemistry Research**, v. 29, n. 3, p. 421–432, 1990.

BATENI, H.; SARAEIAN, A.; ABLE, C. A comprehensive review on biodiesel purification and upgrading. **Biofuel Research Journal**, v. 4, n. 3, p. 668–690, 2017.

BHARATHIRAJA, B. et al. Biodiesel production using chemical and biological methods – A review of process, catalyst, acyl acceptor, source and process variables. **Renewable and Sustainable Energy Reviews**, v. 38, p. 368–382, 2014.

BUDŽAKI, S. et al. Membranska filtracija kao ekološki prihvatljiva metoda pročišćavanja sirovog biodizela. **Kemija u industriji**, v. 69, n. 3–4, p. 175–181, 2020.

CABRERA-JIMÉNEZ, R. et al. Comparing biofuels through the lens of sustainability: A data envelopment analysis approach. **Applied Energy**, v. 307, p. 118201, 2022.

CAO, P. et al. Effect of Membrane Pore Size on the Performance of a Membrane Reactor for Biodiesel Production. **Industrial & Engineering Chemistry Research**, v. 46, n. 1, p. 52–58, 2007.

CAO, P.; DUBÉ, M. A.; TREMBLAY, A. Y. High-purity fatty acid methyl ester production from canola, soybean, palm, and yellow grease lipids by means of a membrane reactor. **Biomass and Bioenergy**, v. 32, n. 11, p. 1028–1036, 2008.

COSTA, M. J. et al. Enzymatic biodiesel production by hydroesterification using waste cooking oil as feedstock. **Chemical Engineering and Processing - Process Intensification**, v. 157, p. 108131, 2020.

DAS, D. et al. Recycling of coal fly ash for fabrication of elongated mullite rod bonded porous SiC ceramic membrane and its application in filtration. **Journal of the European Ceramic Society**, v. 40, n. 5, p. 2163–2172, 2020.

DIMIAN, A. C.; BILDEA, C. S. **Chemical Process Design: Computer-Aided Case Studies**. [s·L: s.n.].

DIN EN 14214. **Liquid petroleum products - Fatty acid methyl esters (FAME) for use in diesel engines and heating applications - Requirements and test methods.** [s·L: s.n.].

DOLAR, D. et al. Removal of anthelmintic drugs and their photodegradation products from water with RO/NF membranes. **Process Safety and Environmental Protection**, v. 90, n. 2, p. 147–152, 2012.

DOS SANTOS, L. K. et al. Experimental factorial design on hydroesterification of waste cooking oil by subcritical conditions for biodiesel production. **Renewable Energy**, v. 114, p. 574–580, 2017.

DUBÉ, M. A.; TREMBLAY, A. Y.; LIU, J. Biodiesel production using a membrane reactor. **Bioresource Technology**, v. 98, n. 3, p. 639–647, 2007.

EN, 12662. Determination of total contamination in middle distillates, diesel fuels and fatty acid methyl esters. In: **Liquid petroleum products.** [s·L: s.n.].

EN, 14538. **FAT AND OIL DERIVATIVES - FATTY ACID METHYL ESTER (FAME) - DETERMINATION OF CA, K, MG AND NA CONTENT BY OPTICAL EMISSION SPECTRAL ANALYSIS WITH INDUCTIVELY COUPLED PLASMA (ICP OES).** [s·L.] Comite Europeen de Normalisation, 2006.

GERPEN, J. VAN. Biodiesel processing and production. **Fuel Processing Technology**, v. 86, n. 10, p. 1097–1107, 2005.

GOG, A. et al. Biodiesel production using enzymatic transesterification – Current state and perspectives. **Renewable Energy**, v. 39, n. 1, p. 10–16, 2012.

GOMES, M. C. S.; PEREIRA, N. C.; BARROS, S. T. D. DE. Separation of biodiesel and glycerol using ceramic membranes. **Journal of Membrane Science**, v. 352, n. 1–2, p. 271–276, 2010.

GOMES, M. C. S.; ARROYO, P. A.; PEREIRA, N. C. Biodiesel production from degummed soybean oil and glycerol removal using ceramic membrane. **Journal of Membrane Science**, v. 378, n. 1–2, p. 453–461, 2011.

GOMES, M. C. S.; ARROYO, P. A.; PEREIRA, N. C. Influence of acidified water addition on the biodiesel and glycerol separation through membrane technology. **Journal of Membrane Science**, v. 431, p. 28–36, 2013.

GOMES, M. C. S.; ARROYO, P. A.; PEREIRA, N. C. Influence of oil quality on biodiesel purification by ultrafiltration. **Journal of Membrane Science**, v. 496, p. 242–249, 2015.

GUO, W.; NGO, H.-H.; LI, J. A mini-review on membrane fouling. **Bioresource Technology**, v. 122, p. 27–34, 2012.

HASSAN, M. H.; KALAM, M. A. An Overview of Biofuel as a Renewable Energy Source: Development and Challenges. **Procedia Engineering**, v. 56, p. 39–53, 2013.

ISO, 15607. **Specification and qualification of welding procedures for metallic materials — General rules**. [s·L: s.n.].

JOSE, A. J.; KAPPEN, J.; ALAGAR, M. Polymeric membranes: Classification, preparation, structure physiochemical, and transport mechanisms. In: **Fundamental Biomaterials: Polymers**. [s·L.] Elsevier, 2018. p. 21–35.

KNOTHE, G. Dependence of biodiesel fuel properties on the structure of fatty acid alkyl esters. **Fuel Processing Technology**, v. 86, n. 10, p. 1059–1070, 2005.

KRISHNASAMY, A.; BUKKARAPU, K. R. A comprehensive review of biodiesel property prediction models for combustion modeling studies. **Fuel**, v. 302, p. 121085, 2021.

LAM, M. K.; LEE, K. T.; MOHAMED, A. R. Homogeneous, heterogeneous and enzymatic catalysis for transesterification of high free fatty acid oil (waste cooking oil) to biodiesel: A review. **Biotechnology Advances**, v. 28, n. 4, p. 500–518, 2010.

LEO, C. P. et al. Potential of nanofiltration and low pressure reverse osmosis in the removal of phosphorus for aquaculture. **Water Science and Technology**, v. 67, n. 4, p. 831–837, 2013.

LEUNG, D. Y. C.; WU, X.; LEUNG, M. K. H. A review on biodiesel production using catalyzed transesterification. **Applied Energy**, v. 87, n. 4, p. 1083–1095, 2010.

LÔBO, I. P.; FERREIRA, S. L. C.; CRUZ, R. S. DA. Biodiesel: parâmetros de qualidade e métodos analíticos. **Química Nova**, v. 32, n. 6, p. 1596–1608, 2009.

LUKOVIC, N.; KNEEVIC-JUGOVIC, Z.; BEZBRADIC, D. Biodiesel Fuel Production by Enzymatic Transesterification of Oils: Recent Trends, Challenges and Future Perspectives. In: **Alternative Fuel**. [s.L.] InTech, 2011.

LV, L. et al. Effect of water on lipase NS81006-catalyzed alcoholysis for biodiesel production. **Process Biochemistry**, v. 58, p. 239–244, 2017.

LV, L. et al. Progress in Enzymatic Biodiesel Production and Commercialization. **Processes**, v. 9, n. 2, p. 355, 2021.

LV, Y.; SUN, S.; LIU, J. Biodiesel Production Catalyzed by a Methanol-Tolerant Lipase A from *Candida antarctica* in the Presence of Excess Water. **ACS Omega**, v. 4, n. 22, p. 20064–20071, 2019.

MA, Y. et al. Biodiesels from microbial oils: Opportunity and challenges. **Bioresource Technology**, v. 263, p. 631–641, 2018.

MANDOLESI DE ARAÚJO, C. D. et al. Biodiesel production from used cooking oil: A review. **Renewable and Sustainable Energy Reviews**, v. 27, p. 445–452, 2013.

MARDHIAH, H. H. et al. A review on latest developments and future prospects of heterogeneous catalyst in biodiesel production from non-edible oils. **Renewable and Sustainable Energy Reviews**, v. 67, p. 1225–1236, 2017.

MEHER, L.; VIDYASAGAR, D.; NAIK, S. Technical aspects of biodiesel production by transesterification—a review. **Renewable and Sustainable Energy Reviews**, v. 10, n. 3, p. 248–268, 2006.

MIBIELLI, G. M. et al. Lab and pilot plant FAME production through enzyme-catalyzed reaction of low-cost feedstocks. **Bioresource Technology Reports**, v. 5, p. 150–156, 2019.

- MOAZENI, F.; CHEN, Y.-C.; ZHANG, G. Enzymatic transesterification for biodiesel production from used cooking oil, a review. **Journal of Cleaner Production**, v. 216, p. 117–128, 2019.
- MOHIDDIN, M. N. BIN et al. Evaluation on feedstock, technologies, catalyst and reactor for sustainable biodiesel production: A review. **Journal of Industrial and Engineering Chemistry**, v. 98, p. 60–81, 2021.
- MONTERO, G. (ED.). Biodiesel- Quality, Emissions and By-Products. 2011.
- MULINARI, J.; OLIVEIRA, J. V.; HOTZA, D. Lipase immobilization on ceramic supports: An overview on techniques and materials. **Biotechnology Advances**, v. 42, p. 107581, 2020.
- NATH, B. et al. Highly efficient renewable heterogeneous base catalyst derived from waste *Sesamum indicum* plant for synthesis of biodiesel. **Renewable Energy**, v. 151, p. 295–310, 2020.
- NEJAD, A. S.; ZAHEDI, A. R. Optimization of biodiesel production as a clean fuel for thermal power plants using renewable energy source. **Renewable Energy**, v. 119, p. 365–374, 2018.
- NORIEGA, M. A.; NARVÁEZ, P. C.; HABERT, A. C. Biodiesel separation using ultrafiltration poly(ether sulfone) hollow fiber membranes: Improving biodiesel and glycerol rich phases settling. **Chemical Engineering Research and Design**, v. 138, p. 32–42, 2018.
- NORJANNAH, B. et al. Enzymatic transesterification for biodiesel production: a comprehensive review. **RSC Advances**, v. 6, n. 65, p. 60034–60055, 2016.
- PADULA, M. L. et al. Dehydration of fatty acid methyl ester mixtures from enzymatic biodiesel using a modified PVDF membrane. **Renewable Energy**, 2022.
- Polishing perspectives: new biodiesel production technologies are likely to require different fuel polishing procedures. **Focus on Catalysts**, v. 2012, n. 7, p. 7, 2012.
- PRICE, J. et al. Scale-up of industrial biodiesel production to 40 m<sup>3</sup> using a liquid



lipase formulation. **Biotechnology and Bioengineering**, v. 113, n. 8, p. 1719–1728, 2016.

RADCLIFF, R.; ZARNADZE, A. **Application of Membrane Technology to the Production of Drinking Water**. Disponível em:

<<https://wcponline.com/2004/08/14/application-membrane-technology-production-drinking-water/>>.

REMONATTO, D. et al. FAME Production from Waste Oils Through Commercial Soluble Lipase Eversa ® Catalysis. **Industrial Biotechnology**, v. 12, n. 4, p. 254–262, 2016.

#### **Resolução ANP Nº 45 DE 25/08/2014.**

ROBERTS, L. G.; PATTERSON, T. J. Biofuels. **Encyclopedia of Toxicology: Third Edition**, p. 469–475, 2014.

RUAN, R. et al. Biofuels: Introduction. **Biomass, Biofuels, Biochemicals: Biofuels: Alternative Feedstocks and Conversion Processes for the Production of Liquid and Gaseous Biofuels**, p. 3–43, 2019.

SALEH, J.; DUBÉ, M. A.; TREMBLAY, A. Y. Effect of soap, methanol, and water on glycerol particle size in biodiesel purification. **Energy and Fuels**, v. 24, n. 11, p. 6179–6186, 2010.

SALEH, J.; TREMBLAY, A. Y.; DUBÉ, M. A. Glycerol removal from biodiesel using membrane separation technology. **Fuel**, v. 89, n. 9, p. 2260–2266, 2010.

SALEH, J.; DUBÉ, M. A.; TREMBLAY, A. Y. Separation of glycerol from FAME using ceramic membranes. **Fuel Processing Technology**, v. 92, n. 7, p. 1305–1310, 2011.

SANDOUQA, A.; AL-HAMAMRE, Z. Economical evaluation of jojoba cultivation for biodiesel production in Jordan. **Renewable Energy**, v. 177, p. 1116–1132, 2021.

SINGH, D. et al. Chemical compositions, properties, and standards for different generation biodiesels: A review. **Fuel**, v. 253, p. 60–71, 2019.

SOKAČ, T. et al. Purification of biodiesel produced by lipase catalysed transesterification by ultrafiltration: Selection of membranes and analysis of membrane blocking mechanisms. **Renewable Energy**, v. 159, p. 642–651, 2020.

SUBRAMANIAM, Y.; MASRON, T. A.; AZMAN, N. H. N. Biofuels, environmental sustainability, and food security: A review of 51 countries. **Energy Research & Social Science**, v. 68, p. 101549, 2020.

SUTHAR, K.; DWIVEDI, A.; JOSHIPURA, M. A review on separation and purification techniques for biodiesel production with special emphasis on Jatropha oil as a feedstock. **Asia-Pacific Journal of Chemical Engineering**, v. 14, n. 5, 2019.

TAJZIEHCHI, K.; SADRAMELI, S. M. Optimization for free glycerol, diglyceride, and triglyceride reduction in biodiesel using ultrafiltration polymeric membrane: Effect of process parameters. **Process Safety and Environmental Protection**, v. 148, p. 34–46, 2021.

THANGARAJ, B. et al. Catalysis in biodiesel production—a review. **Clean Energy**, v. 3, n. 1, p. 2–23, 2019.

**The Novozymes Enzymatic Biodiesel Handbook.** [s·L: s.n.].

TOPARE, N. S. et al. A short review on approach for biodiesel production: Feedstock's, properties, process parameters and environmental sustainability. **Materials Today: Proceedings**, 2021.

TORRES, J. J. et al. Ultrafiltration polymeric membranes for the purification of biodiesel from ethanol. **Journal of Cleaner Production**, v. 141, p. 641–647, 2017.

TORRES, J. J. et al. Biodiesel Purification Using Polymeric Nanofiltration Composite Membranes Highly Resistant to Harsh Conditions. **Chemical Engineering & Technology**, v. 41, n. 2, p. 253–260, 2018.

ULIANA, N. R. et al. Model and simulation of a packed resin column for biodiesel purification. **Renewable Energy**, v. 126, p. 1074–1084, 2018.

WANG, Y. et al. Refining of biodiesel by ceramic membrane separation. **Fuel**

**Processing Technology**, v. 90, n. 3, p. 422–427, 2009.

YADAV, J. S. S. et al. Recovery and Purification Technologies of Biodiesel. In: **Biodiesel Production**. Reston, VA: American Society of Civil Engineers, 2019. p. 453–484.

YANG, Y. et al. An overview of biofuel power generation on policies and finance environment, applied biofuels, device and performance. **Journal of Traffic and Transportation Engineering (English Edition)**, v. 8, n. 4, p. 534–553, 2021.